Journal of Power and Energy Engineering, 2024, 12, 24-59
https://www.scirp.org/journal/jpee
ISSN Online: 2327-5901
ISSN Print: 2327-588X

Numerical Modeling and Technico-Economic Analysis of a Hybrid Energy Production System for Self-Consumption: Case of Rural Area in the Comoros

Fahad Maoulida[1,2], Mohamed Aboudou Kassim[1,2,3*], Rabah Djedjig[1], Ahmed Ihlal[4], Mohammed El Ganaoui[1]

[1]LERMAB, Laboratory of Studies and Research on Wood Material, IUT of Longwy, University of Lorraine, Cosnes-et-Romain, Longwy, France
[2]LEMA, Energy and Applied Mechanics Laboratory, Faculty of Sciences and Techniques, University of Comoros, Moroni, Comoros
[3]IREMIS Institute, University of Mayotte, Mayotte, France
[4]LMER, Laboratory of Materials and Renewable, Faculty of Sciences, University Ibn Zohr BP, Agadir, Morocco
Email: maoulidafahad@gmail.com, *kassim2005k@gmail.com

How to cite this paper: Maoulida, F., Kassim, M.A., Djedjig, R., Ihlal, A. and El Ganaoui, M. (2024) Numerical Modeling and Technico-Economic Analysis of a Hybrid Energy Production System for Self-Consumption: Case of Rural Area in the Comoros. *Journal of Power and Energy Engineering*, **12**, 24-59.
https://doi.org/10.4236/jpee.2024.125002

Received: April 2, 2024
Accepted: May 28, 2024
Published: May 31, 2024

Abstract

This study aims to provide electricity to a remote village in the Union of Comoros that has been affected by energy problems for over 40 years. The study uses a 50 kW diesel generator, a 10 kW wind turbine, 1500 kW photovoltaic solar panels, a converter, and storage batteries as the proposed sources. The main objective of this study is to conduct a detailed analysis and optimization of a hybrid diesel and renewable energy system to meet the electricity demand of a remote area village of 800 to 1500 inhabitants located in the north of Ngazidja Island in Comoros. The study uses the Hybrid Optimization Model for Electric Renewable (HOMER) Pro to conduct simulations and optimize the analysis using meteorological data from Comoros. The results show that hybrid combination is more profitable in terms of margin on economic cost with a less expensive investment. With a diesel cost of $1/L, an average wind speed of 5.09 m/s and a solar irradiation value of 6.14 kWh/m^2/day, the system works well with a proportion of renewable energy production of 99.44% with an emission quantity of 1311.407 kg/year. 99.2% of the production comes from renewable sources with an estimated energy surplus of 2,125,344 kWh/year with the cost of electricity (COE) estimated at $0.18/kWh, presenting a cost-effective alternative compared to current market rates. These results present better optimization of the used hybrid energy system, satisfying energy demand and reducing the environmental impact.

Keywords

Hybrid System, Rural Area Electrification, Comoros, Techno-Economic Analysis, PV-Wind-Diesel-Battery, Meteorological Data, HOMER Energy Pro

1. Introduction

Since the industrial revolution of the 18th century, human activities have resulted in massive emissions in several countries of the world. The exploration of the earth's natural resources caused by human activities from then to the present day challenges us on the extreme effects of climate change recently in many countries of the world [1]. The Comoros is one of the countries facing energy problems and climate change due to its geographical position and insularity in the African continent. Among the main causes of this climate change is the use and production of energy sources, often carried out using fossil fuels such as oil, gas and coal. For any developed or developing country, energy demand is growing rapidly due to the huge consumption of households and businesses [2]. To overcome this problem, the use of other energy sources must be studied [3]. According to the International Energy Agency (IEA), global energy consumption will increase by 37% by 2040. In addition, global electricity demand was expected to increase significantly by 80% over the period 2012-2040. As a result, fossil fuel prices are projected to rise over the next 20 years to reach $215/barrel in 2035. The use of these energy sources generates a very large amount of greenhouse gas emissions, specifically carbon dioxides, which contribute to global warming of our planet [4] [5] [6] [7] [8]. By continuing to use these fossil fuels at this current rate, humanity will experience a huge catastrophe in the coming years [9]. This is why researchers and engineers around the world have proposed [10] [11] the use of green energy sources, which are environmentally friendly, as a solution to overcome this problem. There are several sources of renewable energy, but the most often used and exploited in the world are solar, hydro and wind energy for the daily power of our activities. Mohamad Shahrizal Mohd Noor *et al*. [9] conducted a feasibility analysis of the autonomous supply of renewable energy for a telecommunications tower [12] [13] [14] [15] [16] using Homer in Malaysia with a solar photovoltaic (PV) system. The specificity of their system is that the drinking water production system, which consists of a hybrid solar PV system with a diesel generator, could supply electricity to the load for 24 hours [17] [18] [19]. A review of energy management strategies in hybrid renewable energy systems was studied by Olatomiwa *et al*. [20] with particular attention to energy management strategies used in smart grids. The authors adopted an approach that considers the power of a hybrid renewable energy system in rural areas without connection and with connection to the national electricity grid. According to their main recommendations, it is advisable to develop energies and loads connected directly to these sources. The optimiza-

tion of hybrid systems for the electrification of isolated areas in the Comoros and the design of a hybrid system for powering a telecommunications tower in the Comoros were studied by Kassim *et al*. and Fahad *et al*. [17] [18] [21] [22] [23] [24] with the HOMER software tool combining a PV/Diesel system and a PV/Wind/Diesel system. Their results show that the PV/Diesel/Wind system is more economically profitable and reduces greenhouse gas emissions for environmental protection. Developed countries such as the United Kingdom, the United States, France, Germany, Spain, Australia, Turkey, and Italy have been over-exploited renewable energy as their priorities to replace fossil fuels that harm the global environment and whose number is expected to increase in the future [17]. On the other hand, in developing countries [25] [26] [27] such as the Union of the Comoros lags behind in the use and exploration of renewable energies despite the problems and energy crises that hit these states, due to the cheap price of electricity produced by fossil fuels [28]. The energy intensity of the Comorian economy was USD 0.19 per Megajoule (MJ) in 2017, which is similar to energy intensities observed in other least developed countries [29] Energy needs are dominated by wood and other types of biomass, which met almost half of primary energy needs in 2017. In the Comoros we can see [17] the existence of a tropical climate with an average annual temperature around 29˚C, an average annual wind speed estimated at 5 m/s, the existence of an active volcano that can be exploited with an estimated power of 30 MW as well as exploitable rivers for hydroelectricity. Wood and biomass are used mainly by households and to produce essential oil. Then comes the consumption of diesel, which is also used for electricity generation. Gasoline and kerosene are important fuels for transportation, and many households also rely on kerosene for cooking needs. All petroleum products are imported. Power cuts and load shedding have been ubiquitous. These difficulties have been compounded by the lack of an appropriate strategy and institutional framework, insufficient human resources, the small size of the market and the high cost of diesel. This shows the scale of the energy crisis in the country and the need to find short, medium- and long-term strategies. This urgency is reflected in the decision of the African Development Bank. Despite the government's efforts on renewable energies [17], the share of renewable sources is still low. Therefore, we must insist and encourage the government for maximum exploitation and production of renewable energies and show them that hybrid power plants are reliable than fossil fuel plants and can eradicate once and for all the energy crises that have hit this small island state [8] for more than forty years but will also contribute to the development of the country. It is important to know that renewable energy sources are reliable, as are other sources of electricity generation from fossil fuels [30]. A lot of research in this area shows that renewable energy sources are now cheaper than electricity generation from fossil fuels in terms of leveled energy cost (COE). According to the data presented in **Figure 1**, most Comorian electricity comes from the combustion of fossil fuels. Biomass and petroleum products account for a very large

part of almost all the country's energy production. Given its geographical position, its insularity and one of the countries' most affected by global warming, the Comorian government is very keen to implement renewable energies throughout the country. The use of renewable energy for electricity generation is only 0%, but according to forecasts and state energy policy the country plans to increase this share of renewable energy to 50% by 2030. Several studies are carried out for the use of renewable energies in the Comoros. The most recent include studies by Fahad *et al.* [18] [22] [31] using the HOMER Energy software. With renewable energy like wind and solar PV much cheaper today than they were a decade ago, it's time for the Comorian government and the private sector to invest in these energy sources. Several countries in the world, specifically the most developed nations, have managed to exploit and transform a large part of their sources of electrical energy into renewable energies; developing countries like the Comoros can learn from their experiences. Recently, Fahd and Abdulhakim [17] [32] carried out a techno-economic assessment and optimization of a grid-connected PV and wind generation system for the city of Riadh in Saudi Arabia. Their work explores the feasibility of providing electricity from a hybrid power system (HPS) comprising wind/photovoltaic (PV) and battery. Considering the residential buildings that consume most of the energy in the Saudi network, the city of Riadh is privileged because of its geographical and climatic conditions. The economic analysis is performed by applying the HOMER software because of Net Current Cost (NPC), Energy Cost (COE) and Renewable Fraction for all situations. In addition, to clarify the effect of fuel costs on the system, sensitivity testing is conducted considering two separate tariff rates for residential consumers. The results of the economic analysis show that the current tariff is not economical for the use of HSP in hot and temperate climatic conditions compared [17] to the use of electricity from the grid and the planned tariff shows that it is economical to use HSP compared to electricity from the grid [33]. Husain and Djawad [17] [34] [35] [36] studied an assessment of wind potential in East Jerusalem in Palestine. The authors show that their results can be applied to any study using surface measurements at pre-scissor locations at different altitudes above the ground. In some cases, these energies are much cheaper than fossil fuels, especially from the point of view of energy security. This has been proven in European countries such as Germany, Denmark, Sweden and Norway [28]. This study aims to encourage the use of renewable energy in the country to replace coal, gas and oil. The Union of the Comoros has announced since 2016, a very promising program to develop the use of renewable energies to move from the era of fossil fuels to the era of green energies by 2030. It aims through several programs of international partners to be a pioneer in the production of electricity from renewable energies in the Indian Ocean region. Therefore, solar, wind and geothermal energy is the main objective of the Comorian government to cover 35% of national electricity needs by 2030 [4] [5] [8] [17] [37].

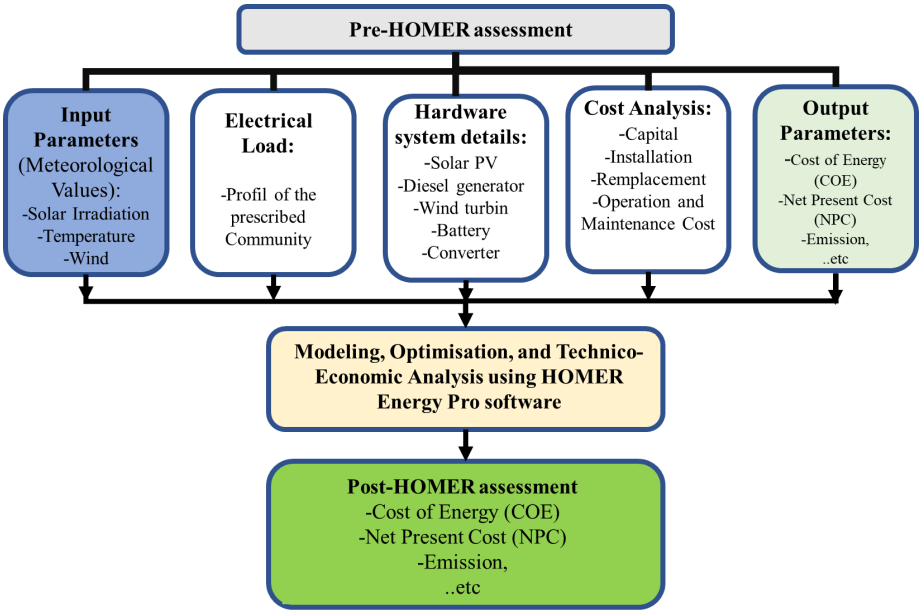

Figure 1. Hybrid energy system design method in HOMER energy pro.

The main objective of this study is to evaluate the performance of an autonomous electrical power generation system, coupling a PV matrix, a wind turbine, and a diesel generator with a storage system composed of batteries to meet the demand of the electric load to supply a village located in rural areas in the Comoros. Propose a simple but flexible method that can be easily applied for the design of an isolated microgrid, thus reducing the complicated computational work for the designer; also carrying out a techno-economic analysis and optimizing hybrid diesel and renewable energy systems. A simple case study is simulated for an autonomous microgrid model, in the commune of Sada djoulamlima north of Ngazidja in the Union of Comoros, to illustrate the effectiveness of the proposed approach using HOMER software [17] [18] [37]. Therefore, the novelty of this research lies in the fact that it focuses on the optimization of a hybrid power plant by improving the accessibility, quality and reliability of renewable electricity supply using techno-economic analysis.

2. Methodology

The assessment of renewable energy projects typically requires the application of relevant criteria to on-site location data to appropriately examine the operational behavior of all potential scenarios. In this research, the following analytical framework was used [38] [39]:

- Location specification
- The modeling data require:
  - ✓ Average electric load demand.
  - ✓ Daily radiation and clearness index at the location.
  - ✓ Wind velocity data.
  - ✓ The daily temperature at the location.

✓ System architecture.

The information collected was fed into the HOMER software for a simulation process. First, the simulation was carried out for different scenarios depending on their electricity consumption, the combination of renewable energy technologies used and the type of system [40].

- Analysis of output results

After the simulation, the payback time, component costs, net present cost and present value of each scenario were analyzed to select the best investment strategy.

The collected data from the site was analyzed and evaluated using various criteria. Each of these criteria was carefully examined and studied to fully characterize the overall design of the system, with a specific focus on the selection of renewable energy components [41]. The Hybrid Optimization Model for Electric Renewable (HOMER) Pro software was utilized for this analysis [42]. Developed by the U.S. Department of Energy, under the National Renewable Energy Laboratory (NREL), in 1992, HOMER Pro is a widely used tool for performing techno-economic analysis of renewable energy systems for off-grid applications [43]-[48]. The HOMER Grid version of the software was created to address the growing need for modeling behind-the-meter projects, such as solar systems with storage or more complex systems, such as wind, emergency generators, and combined heat and power [34] [35]. The software allows for the integration of technical and economic data into a single model, enabling users to perform complex calculations, assess the value of self-consumption, and optimize the system design. It also enables users to analyze multiple component options, evaluate cost competitiveness points for alternative technologies, and minimize project risk by identifying the most cost-effective design. Additionally, it allows for the replication of real-world performance which helps system designers and optimizers make better decisions.

3. Geographical Presentation of Comoros Archipelago

The Comoros archipelago is located in the Indian Ocean, north of the Mozambique Channel, between East Africa and the west coast of Madagascar. It consists of four volcanic islands: Grande Comore (Ngazidja) which is the largest island with an area of 67 km in length and 27 km in width, for a total area of 1146 km^2, Anjouan (Ndzouwani) is the second federal state of the Union of Comoros, Moheli (Mwali) is the third federated state of the Union of the Comoros and one of the four main islands that make up the Comoros archipelago [36] [37]. It is the smallest and most touristic of the three islands of the Union of the Comoros. Finally, Mayotte (Maoré) is the oldest island of the four islands, located 295 km west of Madagascar and 67 km southwest of the island of Anjouan. Mayotte is composed of several islands and islets covered with vegetation, it is under French administration and became a French department in 2009, however it's not considered as part of Comoros. The Comoros has a total area of 2234 km^2 and an estimated population of 1071229 inhabitants (without Mayotte) according to the census of

2018. The densest island is Anjouan with 517 inhabitants/km^2, followed by Grande Comoros with 240 inhabitants/km^2, and finally Moheli with 99 inhabitants/km^2.

Energy Problems in the Union of the Comoros

The Comoros has been grappling with a persistent energy crisis for over four decades, with recurrent power outages affecting the entire country. These outages are caused by a variety of factors, including mechanical problems and inadequate maintenance within the energy company, insufficient financial support from SONELEC, as well as social, political, geographical, and economic issues.

In 2016, there was a severe electricity crisis in Mwali and Ngazidja, resulting in prolonged power outages and electricity rationing. One of the main cultural challenges faced in this regard is related to electricity billing [17] [22] [24] [29] [49] [50] [51] [52]. Many consumers tend not to pay their full bills, primarily due to issues with metering methods, illegal connections, or social status, which poses significant challenges for revenue collection efforts. The percentage of energy mix and consumption for the year 2017 is illustrated in **Figure 2** [29] [52].

Before 2020, electricity production in the Comoros was mainly from diesel thermal power plants. In the table (see **Table 1**), we can see the names of the different plants and their respective capacities [31].

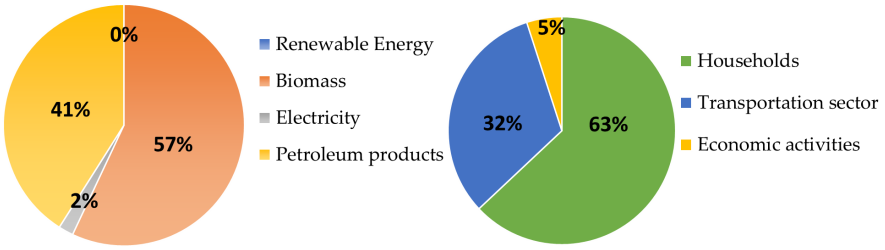

(a). National Energy package (b). Energy consumption

Figure 2. Bouquet and National energy consumption in 2017 [52].

Table 1. Different power plants and their capacities [31].

Power plants	Nb. ofgenerators	Capacity (MW)
	Grande Comore (Ngazidja)	
Voidjou Power Plant	10 Caterpillar generator sets	16
Itsambouni Power Plant	5 Caterpillar Groups	2.8
	Moheli (Mwali)	
Fomboni Power Plant	5 groups including 2 Caterpillar, 2 Mitsubishi and 1 SDMO	5.38
	Anjouan (Ndzuwani)	
Trenani Power Stations, Lingoni	7 Caterpillar groups, Micro-hydro.	6.3
Total		30.48

The country is lagging far behind in terms of renewable energy sources. Moreover, a recent study on renewable energy options in the Comoros (see **Table 2**) highlighted the possibility of a 10 MW geothermal power plant and a 15 MW public solar farm in Grande Comore. However, a 5 MW hydroelectric plant and a 6 MW wind farm can be installed in Anjouan. In Moheli, 27 kW of hydroelectric power plant are exploitable [31]. Based on the levelized cost of energy (LCOE) of each technology, the Geological Office of the Comoros proposed a 5 MW solar farm and a 10 MW geothermal power plant in Grande Comore. These facilities could provide a short-term energy solution for the island but combining them with existing fossil fuel systems to make the energy mix could be a long-term solution for energy stability in the Comoros.

Although the Comoros currently produces all its energy from diesel power plants, several studies highlight the possibility of energy independence through renewable energies, particularly solar potential as shown in **Figure 3**. Solar energy has been successful in private homes, stand-alone photovoltaic systems, and the distribution of solar micro-power plants [53].

Table 2. Comoros' renewable energy potential [52].

Energy source	Comoros	Ngazidja	Ndzouwani	Mwali
Wind generator	15 MW	-	6 MW	-
Hydroelectricity	1 MW	-	5 MW	27 kW
Solar	5 kWh/m^2/day	5 MW	-	-
Geothermal energy	-	10 MW	-	-
Biomass	-	5 MW	-	-

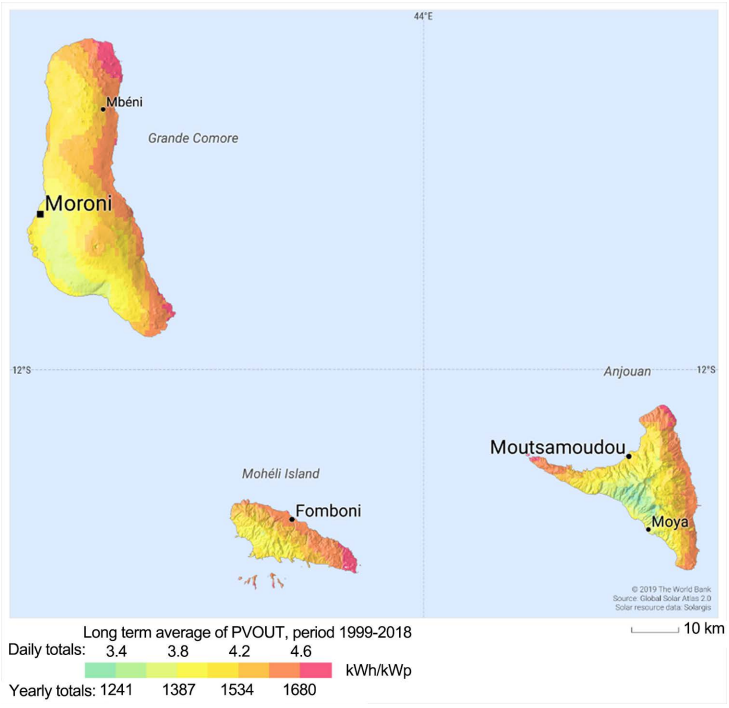

Figure 3. Photovoltaic electricity potential (Solar field) of the Comoros [54].

In 2020, the country began registering its first photovoltaic power plants. In Pomoni in the commune of Moya in the Sima region on the island of Anjouan, a photovoltaic solar power plant has been built, located in a plot of five hectares, now under the management of SONELEC. With this additional capacity, Ndzuani now has 6 MW since the plant has a capacity of 4 Mw and will cover 40% of the island's electricity needs. In 2022, a photovoltaic plant in Foumbouni in the south of the island of Ngazidja was built with a power of 3 Mw or 13% of production. In Moheli, a solar power plant of 250 kW or 0.25 MW is installed. Other projects are under way throughout the country.

4. System Modeling

4.1. Site of Implantation and Demand of the Electrical Load

The village of Koua is located in the north of Grande Comore, more precisely in the commune of Sada Djoulamlima, which consists of three villages (Koua, Oellah, and Wemani) as shown in Figure 4. To carry out this project, we conducted surveys in the commune to determine the electrical load of a typical family home before making an estimate for the entire community.

Table 3 shows the energy consumption of a typical family member of the village. The demand for the electric charge is available throughout the village, which has 130 to 200 families on average with 5 to 6 people average member in each family and 800 to 1000 inhabitants in 2021. According to surveys already done, the whole village consumes 1603.60 kWh per day, with an average peak load of 143.16 kW as shown in Figure 5. To electrify this village, we considered it necessary to install a hybrid system composed of solar photovoltaics, a wind turbine, a diesel generator, and storage batteries with the objective in this work of optimizing renewable sources and minimizing the intervention of the diesel generator. Energy demand assumptions were based on historical data and local

Figure 4. Location of the site of implantation.

Table 3. Daily charge of a typical village household.

Electrical appliance	Nb.	Power P (W)	Running time (hour)	Energy consumed. (kWh/day)
Hi-Fi system	1	80	5	0.4
Fans	1	40	10	0.4
TV Sallon	1	100	8	0.8
Radio D500	1	10	10	0.1
Light bulbs	3	40	6	0.72
Rice cooker	1	500	1	0.5
LED	2	8	6	0.096
Iron	1	750	1	0.75
Refrigerator	1	150	24	3.6
Freezer	1	110	24	2.64
Water heater	1	2400	1	2.4
Total	-	4188	-	12.406

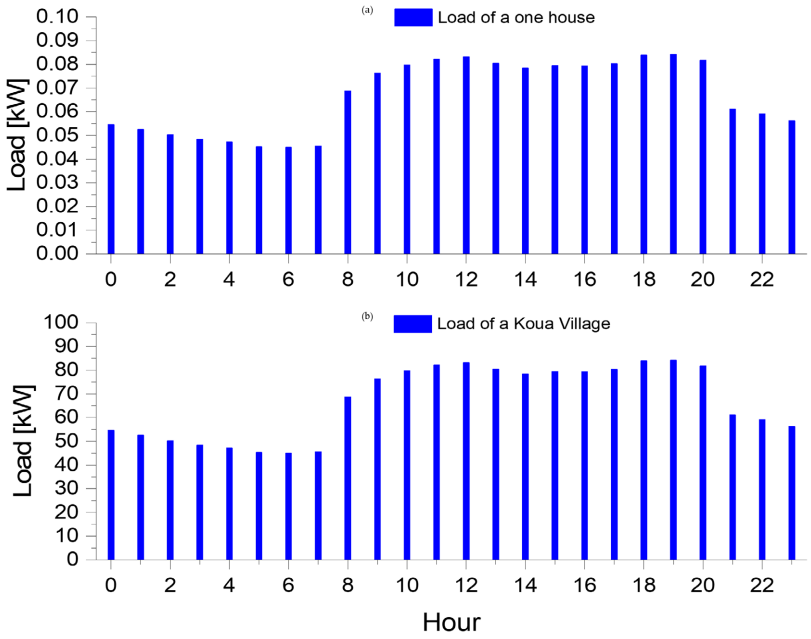

Figure 5. Electrical load profile for a typical house and village.

surveys, taking into account seasonal variations and demand peaks to optimize the system design.

this hybrid energy system, some input data must be calculated to determine which system is optimized with the best efficiency and lowest cost.

4.2. The Site Weather Data

The average daily sunshine north of Ngazidja is estimated at 10 hours of time per day with an average power between 5 to 6.5 kW/m^2/day of production. Weather data from Ngazidja between 1961 and 2018 show effective sunshine regardless of

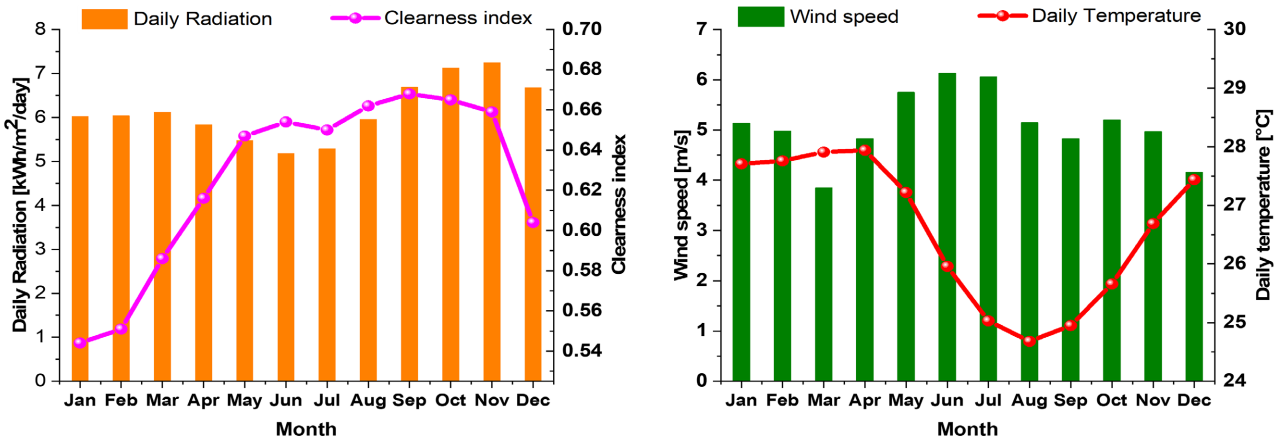

(a). Solar Radiation and clearness index

(b). Wind speed and temperature

Figure 6. Village weather data.

the month or season. The Comoros archipelago also receives a very high rate of solar radiation. These values show that the country has strong solar radiation capable of powering photovoltaic and solar thermal installations [17]. In the case of this study, the average solar irradiation of the village is 6.14 kWh/m²/day. Indeed, the HOMER software tool directly retrieves the clarity index via the information present on the latitude of the site studied for this village located in a rural area (**Figure 6(a)**).

The source of the wind turbine considered is none other than the wind speed. In our case, we note that throughout the year the lowest speed is observed in March with 3.7 m/s while the highest is obtained in June with a value of 6.3 m/s (**Figure 6(b)**). The average temperature varies between 24.5˚C to 28.5˚C throughout the year as shown in **Figure 6(b)**. Note that these data are obtained directly in the NASA database and are justified in relation to the data of the ANACEM (National Agency of Civil Aviation and Meteorology) of the Union of the Comoros [17].

4.3. Architecture of the Proposed System

Before simulating the hybrid system in Homer Energy, we first design the architecture of the system. In our case, the system is composed of photovoltaic solar panels, a wind turbine, a diesel generator, storage batteries and converters which consist of transforming direct current into alternating current. The photovoltaic system chosen is CS6U-340M from Canadian Solar with an efficiency of 17.49%, a ground reflectance of 20%, a decommissioning factor of 80% and a service life of 25 years. The proposed wind turbine has a power of 10 kW, a hub height of 24 m and a lifespan of 20 years. The selected battery is the OPzS 3780 DC type with a nominal voltage of 2 V, a rated capacity of 1 kWh, a capacity ratio of 0.403, a round trip efficiency of 85%, a maximum state load of 100%, a minimum state load of 40%, a flow rate of 7862.40 kWh and a service life of 20 years. At the same time, the converter of the selected

system has a relative capacity of 100%, an input efficiency of the inverter and rectifier of 95% and a service life of 25 years [17] [55] [56]. We selected the components of the hybrid system based on their cost, efficiency, reliability and compatibility. Environmental criteria and resilience to local climatic conditions also played a crucial role in this choice.

Component reliability is critical, given the harsh environmental conditions. A maintenance plan adapted to the geographical remoteness of the site has been developed to ensure the sustainability of the system.

Here is the architecture simulated on HOMER Energy Pro in order to electrify the village in an optimal way. HOMER Pro was chosen for its ability to integrate technical and economic data, enabling accurate optimization and economic analysis of hybrid energy systems under isolated conditions.

The equipment is collected in the catalog provided by the software. **Figure 7** shows the architecture diagram of the proposed system. Detailed information on the system is presented in **Table 4**. In this first scenario, photovoltaic solar panels, wind turbines, a diesel generator and a battery energy storage system feed the load, and all systems are not connected to the power grid [17] [57] [58].

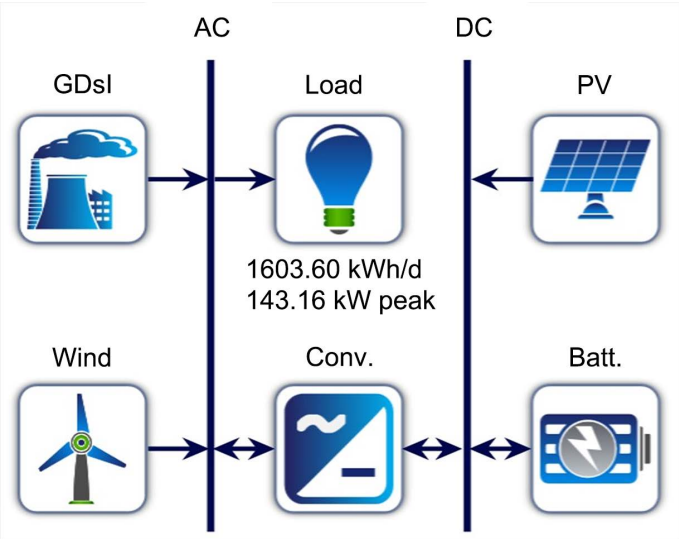

Figure 7. Proposed system architecture(HOMER Energy Pro).

Table 4. The component of the proposed system architecture.

Component	Name	Capital ($)	Replacement ($)	O&M Cost ($)	Lifetime (year)
Diesel Generator	Diesel 50	500	500	0.030/op hour	25 years
PV	CS6U-340M	800	750	5/year	25 years
Wind Turbine	WES 80	50,000	50,000	50/year	20 years
Converter	Converter	300	250	0/year	20 years
Storage	Kinetic Battery	300	250	3/year	20 years

5. Modeling Hybrid System Components

5.1. Diesel Generator and Fuel Modeling

In this study, the AC type diesel generator (DG) can generate at rated power. Thus, the observed excess energy can participate in the charge of a battery in general. Indeed, the DG is designed in such a way that it operates between 75 and 100% of the assessment in kW by operating with a storage system or other renewable energy sources. To make a better comparison between the system and a feasibility system, we included it in the simulation [17]. The mathematical equations for modeling the system are derived within the HOMER Energy Pro software model [43] [59].

A very important element of this study is fuel. From the generator inputs, one can determine the fuel curve which is described as the amount of fuel that the generator consumes to produce electricity. HOMER Pro assumes that the fuel curve is a straight line. The following equation gives the fuel consumption of the generator in units/h as a function of its electrical power [59]:

$$F = F_0 \cdot Y_{gen} + F_1 \cdot P_{gen} \tag{1}$$

where is F_0 the fuel curve intercept coefficient [units/hr/kW], F_1 the fuel curve slope [units/hr/kW], Y_{gen} rated capacity of the generator [kW] and P_{gen} the electrical output of the generator [kW]. In HOMER Energy Pro, we define the generator's electrical efficiency as the electrical energy coming out divided by the chemical energy of the fuel going in. The following equation gives this relationship [59]:

$$\eta_{gen} = \frac{3.6 \cdot P_{gen}}{\dot{m}_{fuel} \cdot LHV_{fuel}} \tag{2}$$

where is P_{gen} the electrical output [kW], $\dot{m}_{fuel}$ the mass flow rate of the fuel [kg/hr] and LHV fuel the lower heating value (a measure of energy content) of the fuel [MJ/kg]. The factor of 3.6 arises because 1 kWh = 3.6 MJ. The mass flow rate of the fuel is related to F, the generator's fuel consumption, but the exact relationship depends on the units of the fuel. If the fuel units are kg, then $\dot{m}_{fuel}$ and F are equal, so the equation for $\dot{m}_{fuel}$ is as follows [59]:

$$\dot{m}_{fuel} = F = F_0 \cdot Y_{gen} + F_1 \cdot P_{gen} \tag{3}$$

If the fuel units are L, the relationship between $\dot{m}_{fuel}$ and F involves the density. The equation for $\dot{m}_{fuel}$ is as follows:

$$\dot{m}_{fuel} = \rho_{fuel}\left(\frac{F}{1000}\right) = \frac{\rho_{fuel}\left(F_0 \cdot Y_{gen} + F_1 \cdot P_{gen}\right)}{1000} \tag{4}$$

where ρ_{fuel} is the fuel density [kg/m^3]. If the fuel units are m^3, the factor of 1000 is unnecessary, and the equation for $\dot{m}_{fuel}$ is as follows [59]:

$$\dot{m}_{fuel} = \rho_{fuel} F = \rho_{fuel}\left(F_0 \cdot Y_{gen} + F_1 \cdot P_{gen}\right) \tag{5}$$

Table 5 provides an overview of the various characteristics and essential parameters of diesel fuel.

Table 5. Physical characteristics of the diesel fuel [17].

Fuel properties	Value
Lower heating value	43.2 MJ/kg
Density	820 kg/m^3
Carbon content	88%
Sulfur content	0.4%
Fuel cost max	$ 1
Fuel cost min	$ 0.98

If the fuel units are L, the efficiency equation becomes:

$$\eta_{gen} = \frac{3600 \cdot P_{gen}}{\rho_{fuel}\left(F_0 \cdot Y_{gen} + F_1 \cdot P_{gen}\right) \cdot LHV_{fuel}} \tag{6}$$

If we divide numerator and denominator by Y_{gen}, the capacity of the generator, and define a new symbol p_{gen} for the relative output of the generator ($p_{gen} = P_{gen}/Y_{gen}$) then the efficiency equation becomes [59]:

$$\eta_{gen} = \frac{3600 \cdot p_{gen}}{\rho_{fuel}\left(F_0 + F_1 \cdot p_{gen}\right) \cdot LHV_{fuel}} \tag{7}$$

This equation gives the efficiency of the generator as a function of its relative output. HOMER Energy plots this relationship in the efficiency curve in the Generator Inputs window when the fuel units are L. If the fuel units are m^3, the efficiency equation becomes [59]:

$$\eta_{gen} = \frac{3.6 \cdot p_{gen}}{\rho_{fuel}\left(F_0 + F_1 \cdot p_{gen}\right) \cdot LHV_{fuel}} \tag{8}$$

Finally, if the fuel units are kg, the efficiency equation becomes [59]:

$$\eta_{gen} = \frac{3.6 \cdot p_{gen}}{\left(F_0 + F_1 \cdot p_{gen}\right) \cdot LHV_{fuel}} \tag{9}$$

5.2. Solar Photovoltaic

In a photovoltaic system, a cutting factor, which is a scale factor applied to the production of the PV panel and a cutting factor of 90% for the component, is added to account for losses and those attributable to fouling of the PV panel [18] [31] [60]. The energy production of the PV generator is determined using the following formula [61]:

$$P_{PV} = Y_{PV} f_{PV} \left(\frac{\bar{G}_T}{\bar{G}_{T,STC}}\right)\left[1 + \alpha_P\left(T_C - T_{C,STC}\right)\right] \tag{10}$$

where is Y_{PV} : the rated capacity of the PV array, meaning its power output under standard test conditions [kW],f_{PV} the PV derating factor [%], $\bar{G}_T$ the solar radiation incident on the PV array in the current time step [kW/m^2],

$\bar{G}_{T,STC}$ the incident radiation at standard test conditions [1 kW/m²], α_P The temperature coefficient of power [%/˚C], T_C the PV cell temperature in the current time step [˚C] and $T_{C,STC}$ the PV cell temperature under standard test conditions [25˚C].

If, on the PV page, you choose not to model the effect of temperature on the PV array, HOMER assumes that the temperature coefficient of power is zero, so the equation above is simplified [61]:

$$P_{PV} = Y_{PV} f_{PV} \left(\frac{\bar{G}_T}{\bar{G}_{T,STC}} \right) \tag{11}$$

The equivalent diagram of a photovoltaic cell includes a current generator that models illuminance and a diode in parallel that models the PN junction, but the real equivalent diagram considers the parasitic resistive effect due to manufacturing, it is represented on the equivalent diagram by two resistors **Figure 8** [62].

The current source generates a current I_{ph} proportional to the illuminance H [w/m²]. The shunt resistor R_P characterizes the leakage current at the junction and the resistor R_s represents the various contact and connection resistors. The current I supplied by the cell is the difference between the current I_{ph} and the current of the diode I_D *[17]*.

$$I = I_{ph} - I_D - I_p \tag{12}$$

$$I = I_{ph} - I_D = I_{ph} - I_0 \left(\exp \frac{e(V + R_s I)}{mkT_c} - 1 \right) - \frac{V + R_s I}{R_p} \tag{13}$$

where: I_o is the saturation current of the unlit junction, I_c the current of the cell, e the charge of the electron (1.602×10^{-19} C), K the Boltzmann constant (1.381×10^{-23} J/K), T_c is the junction temperature of the photovoltaic cell, m the ideality factor of the junction, V the voltage across the cell, R_s the series resistor and R_P the shunt resistor [31].

$$I_0 = \exp \left(\frac{-E_g}{kT_c} \right) \tag{14}$$

where $V_T = k \cdot T_c / e$ is the thermal tension, E_g is the bandgap energy for a given semiconductor material. It is almost constant and I_0 is therefore a function of temperature. Ideally, we can neglect R_s and I in front of V, then work with a simplified model [62]:

$$I = I_{ph} - I_D = I_{ph} - I_0 \left(\exp \left(\frac{e.V}{m \cdot k \cdot T_c} \right) - 1 \right) - \frac{V}{R_p} \tag{15}$$

The influence of temperature is important and has consequences for the design of photovoltaic panels and systems. Temperature is an essential parameter since cells are exposed to solar radiation, which can heat them. In addition, part

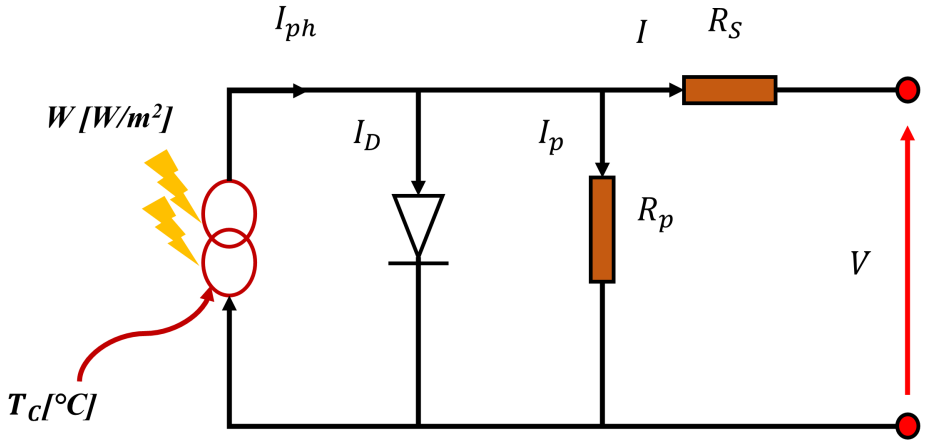

Figure 8. Electrical diagram equivalent of a solar cell.

of the absorbed radiation is not converted into electrical energy [63]: it is dissipated in the form of heat; this is why the cell temperature (T_c) is always higher than the ambient temperature T_a [62].

$$T_c = T_a + H_{in} \cdot \frac{NOCT - 20}{1000} \tag{16}$$

With T_a an ambient temperature (˚C), H_{in} Solar irradiation on the inclined-plane (w/m²) and $NOCT$ the operating temperature of the cell which is defined as the temperature of the cell when the module operates under the following conditions of Solar Irradiation of 1000 W/m², Spectral Distribution of AM1.5 Ambient Temperature of 25˚C and Wind Speed greater than 1 m/s. **Figure 9(a)** shows that the tension of a cell decreases sharply with temperature. The higher the temperature, the less efficient the cell. On the other hand, the current increases slightly in intensity; however, this increase remains negligible at the point of maximum power. In **Figure 9(b)**, the increase in temperature also results in a decrease in the maximum available power (the order of (5×10^{-3} w/k per cm² of the cell) [64].

The electrical energy produced by a cell depends on the illuminance it receives on its surface. The previous equations are only valid for an optimal mode of operation. To generalize our calculation for different illuminances and temperatures, we use the model that moves the reference curve to new locations [31] [62].

$$I_{sc} = I_{scr} \cdot \frac{H}{1000} \tag{17}$$

The reference short-circuits current, H the global solar irradiation. In the same way as temperature, the PN junction reacts differently depending on the energy it receives. The more energy it receives, the more it returns, but always with a very low efficiency coefficient of around 15%. The variation in characteristics is shown in **Figure 9(c)** and **Figure 9(d)**, depending on weather conditions. We get different curves with different maximum powers during the same day.

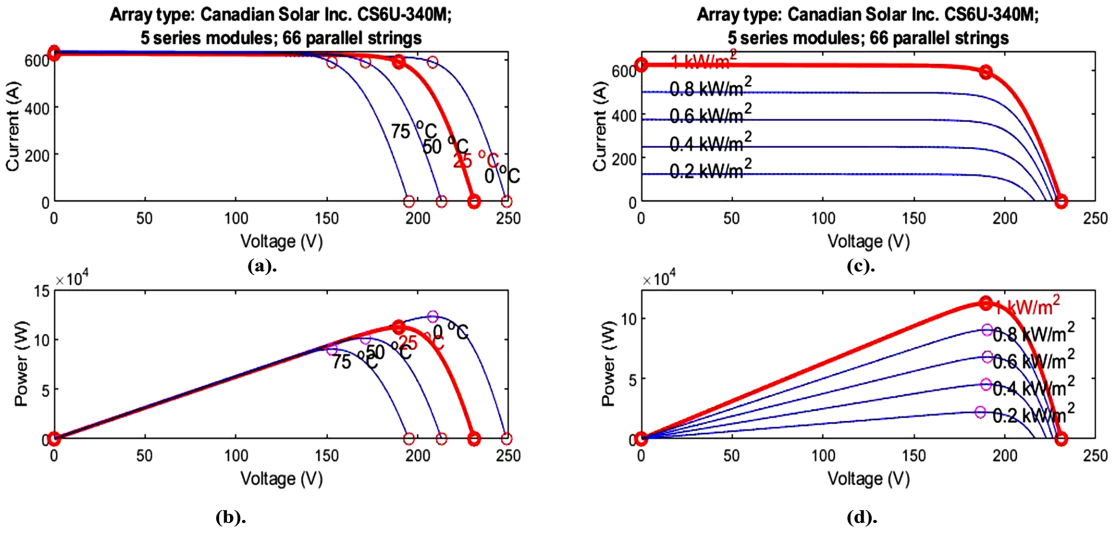

Figure 9. Influence of temperature and radiation on PV module Type CS6U-340M.

$$U_{hub} = U_{anem} \cdot \frac{\ln\left(\frac{Z_{hub}}{Z_0}\right)}{\ln\left(\frac{Z_{anem}}{Z_0}\right)} \tag{18}$$

where U_{hub} is the wind speed at the hub height of the wind turbine [m/s], U_{anem} the wind speed at anemometer height [m/s], Z_{hub} the hub height of the wind turbine [m], Z_{anem} the anemometer height [m], Z_0 the surface roughness length [m] and ln(..) the natural logarithm. If you choose to apply the power law, HOMER calculates the hub height wind speed using the following equation [17] [65]:

$$U_{hub} = U_{anem} \cdot \left(\frac{Z_{hub}}{Z_{anem}}\right)^{\alpha} \tag{19}$$

where : U_{hub} is the wind speed at the hub height of the wind turbine [m/s], U_{anem} the wind speed at anemometer height [m/s], Z_{hub} the hub height of the wind turbine [m], Z_{anem} the anemometer height [m] and α the power law exponent. Power curves typically specify wind turbine performance under conditions of standard temperature and pressure (STP). To adjust to actual conditions, HOMER multiplies the power value predicted by the power curve by the air density ratio, according to following equation [32] [65] [66]:

$$P_{WTG} = \frac{\rho}{\rho_0} \cdot P_{WTG,ST} \tag{20}$$

where P_{WTG} is the wind turbine power output [kW], $P_{WTG,STP}$ the wind turbine power output at standard temperature and pressure [kW], ρ the actual air density [kg/m^3], and ρ_0 the air density at standard temperature and pressure (1.225 kg/m^3) [66]. **Figure 10** shows the maximum operating power of the wind turbine. With a wind speed of 15 m/s, the wind turbine reaches the power of 10 kW which is the operating power.

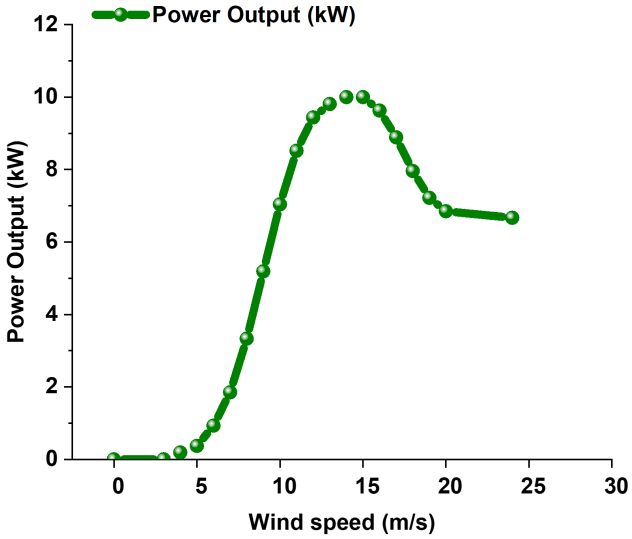

Figure 10. Wind turbine power curve.

5.3. Converter

A converter is a device that converts electrical energy from direct current to alternating current during reversal and from alternating current to direct current during straightening [17]. The size of the converter refers to the capacity of the inverter or the largest amount of alternating current that the device can generate by reversing continuous energy. The rectifier capacity is expressed as a percentage of the inverter capacity, which is the largest amount of DC energy the unit can produce by straightening AC energy. The inverter and rectifier capacities are continuous, without overvoltage, and the device can handle the load for as long as needed, according to the software. For this, the inverter must be able to synchronize with the frequency of alternating current, which is lacking in some inverters [17]. Converter reversal and straightening efficiencies are the ultimate physical attributes of the converter, which the software expects to remain constant. The economic characteristics of the converter are the investment and replacement costs in dollars per year and the expected life of the converter in years [17].

5.4. Storage Battery

HOMER models a single battery as a device capable of storing a specific amount of energy in direct current with fixed energy efficiency, subject to limits on how quickly it can be charged or drained, as well as how much energy can flow through it before it needs to be replaced. The program implies that the characteristics of the battery remain constant over time and are not affected by environmental influences such as temperature. A group of one or more separate batteries is called a "battery bank". The software predicted the life of the battery bank by simply monitoring the amount of energy passing through it, since the flow rate of the battery life is independent of the depth of the cycle in this situation. The life of

the battery bank in years is calculated by the program based on the following equation [43] [67]:

$$R_{batt} = MIN\left(\frac{N_{batt}Q_{lifetime}}{Q_{thrpt}}, R_{batt,f}\right) \tag{21}$$

where R_{batt} is the life of storage bank(year), N_{batt} storage bank number of batteries, $Q_{lifetime}$ is the single storage lifetime throughput (kWh), Q_{thrpt} is storage throughput annually (kWh/year), and $R_{batt,f}$ is storage float life (year). The cyclic energy expenditure through the storage bench is known as the cost of battery wear and tear of the battery. Suppose that storage characteristics show that throughput is a constraint on lifetime. In this case, the program estimates that the storage bench will need to be replaced when its total throughput equals the throughput of its lifetime. Therefore, the storage bench approaches its necessary replacement with each kWh of flow. The software uses the following calculation to calculate the cost of storage wear [30] [39] [43]:

$$C_{bw} = \frac{C_{rep,batt}}{N_{batt} \cdot Q_{lifetime} \cdot \sqrt{\eta_{rt}}} \tag{22}$$

where $C_{rep,batt}$ is storage bank replacement cost ($), N_{batt} is storage bank number of batteries, $Q_{lifetime}$ is single storage lifetime throughput (kWh), and η_{rt} is storage roundtrip efficiency (fractional).

6. Economic Analysis and Interest Rates

To make a techno-economic study of the system, it is necessary to consider certain economic data including the life of the project, the nominal discount rate, the expected inflation rate [63]. The economic data required for this analysis are presented in **Table 6**.

Other information considered in this project is the annual real interest rate, also known as the real interest rate or simply the interest rate. The discount rate is used to convert one-time costs into annualized expenses [17]. The following equation is used to determine the relationship between the annual real interest rate and the annual nominal interest rate [17] [63]:

$$i = \frac{i' - f}{1 + f} \tag{23}$$

where i is the real interest rate, i' is the nominal interest rate (the rate at which the project can obtain a loan) and f is the annual inflation rate in this equation. Thus, for system optimization HOMER Energy Pro needs the lifespan, initial investment cost, replacement cost, maintenance, and labor of each component to calculate the net project cost (*NPC*) and the cost of energy (*COE*) of the system to meet load demand. The total net present cost (*NPC*) of a system is the present value of all costs incurred by the system over its lifetime, less the present value of all revenues it earns over its lifetime. This value can be determined by the following expression [17]:

Table 6. Economic input data.

Description	Value	Unit
Currency	US Dollar	$
Diesel price	1	$/L
Nominal Discount rate	6.6	%
Expected inflation rate	2.0	%
Project lifetime	25	Year

$$C_{NPC} = \frac{C_{ann,tot}}{CRF\left(i, R_{proj}\right)} \tag{24}$$

In this equation $C_{ann,tot}$ is the total annualized cost (USD/year), CRF is the capital recovery factor, i is the real interest rate (%), and R_{proj} is project lifetime (year) (25 years in this study). The capital recovery factor is a ratio used to assess an annual present value (a series of equal annual cash flows). The capital recovery factor's equation is [43]:

$$CRF\left(i, N\right) = \frac{i\left(1+i\right)^{N}}{\left(1+i\right)^{N}-1} \tag{25}$$

where i is the real interest rate (%) and N is the number of years. HOMER calculates the discount factor f_d using the following equation [63]:

$$f_d = \frac{1}{\left(1+i\right)^{N}} \tag{26}$$

With N representing the year the project was developed. HOMER defines levelized cost of energy (COE) as the average cost per kWh of useful electrical energy produced by the system. To calculate the COE, HOMER divides the annualized cost of generating electricity (the total annualized cost minus the cost of the heat load) by the total electrical load served, using the following equation [17] [68]:

$$COE = \frac{C_{ann,tot} - C_{boiler} H_{served}}{E_{served}} \tag{27}$$

where, $C_{ann,tot}$ is the total annualized cost of the system [$/yr], C_{boiler} boiler marginal cost [$/kWh], H_{served} total thermal load served [kWh/yr] and E_{served} total electrical load served [kWh/yr]. The second term in the numerator is the portion of the annualized cost that results from serving the thermal load. In systems, such as wind or PV, that do not serve a thermal load ($H_{thermal}$ = 0), this term is zero. In our case, equation 26 becomes [17] [68]:

$$COE = \frac{C_{ann,tot}}{E_{served}} \tag{28}$$

The COE is a convenient metric with which to compare systems, but HOMER does not rank systems based on COE [17]. The software uses the recovery value, which is the value of a component of the electrical system that is still usable at

the end of the project's life, to calculate the value of each component after the project's lifecycle [69]:

$$S = C_{rep} \frac{R_{rem}}{R_{comp}} \tag{29}$$

where S is the salvage value, C_{repis} the component replacement cost, R_{remis} the remaining component life, and R_{compis} the component lifetime. The annualized total cost of a component is calculated by multiplying the net present cost by a factor, called the capital recovery factor. This factor distributes the cost evenly over the project's life and results in the same net present cost as the component's actual cash flow sequence [70]:

$$C_{ann,tot} = CRF\left(i, R_{proj}\right) \cdot C_{NPC,tot} \tag{30}$$

where $C_{NPC,tot}$ is the current net total cost (USD), i is the annual real discount rate (%), R_{proj} is the life of the project (year), and CRF is a function returning the capital recovery factor. The leveled cost of energy is calculated using the total annualized cost [33] [70].

7. Results

Our system has been simulated under various scenarios, considering variations in load profile, component cost and size, system constraints, control strategy and system economy. HOMER eliminates any infeasible combinations and ranks the feasible systems based on their net present cost. This software has many features, but its main functionalities are feasibility studies and techno-economic studies of microgrids or distributed off-grid or grid-connected energy systems and allows for modeling and optimizing low-cost renewable energy systems and risk mitigation techniques. It demonstrates how to combine fossil energy production with renewable energy, storage, grid resources (if available) and load control based on a techno-economic analysis. In a single simulation run, the program evaluates and optimizes power system architecture, load profiles, components, fuel prices and environmental factors, simulating the operation of a hybrid microgrid or distributed energy system for one year.

7.1. Results by Optimisation

A study was conducted in the village of Koua in the Union of Comoros (11˚24.3'S, 43˚20.9'E) which yielded four potential architectural options for a hybrid power plant. The system would use 1603.60 kWh/day and have a peak power of 143.16 kW. The simulation software Homer generated a list of system configurations based on their lowest cost of energy and net present cost. Different configurations were considered and the optimal design that best fits the village's needs was chosen. The details of the chosen optimized components can be found in **Table 7**, with the reference case (**Figure 11(d)**) in light green. The specifics of the optimized system design are also outlined in **Table 7**. These optimization results are provided by the HOMER Energy software after validation of various parameters.

Table 7. Optimization results of the proposed system.

Rank	PV [kW]	Wind Nb.	Generator [kW]	Battery Nb.	Converter [kW]	NPC [$]	COE [$]	Ren Frac [%]
1	1500		0	500	100	$1.60M	$0.175	100
2	1500	1	0	500	100	$1.66M	$0.181	100
3	1500		50	500	100	$1.66M	$0.182	99
4	1500	1	50	500	100	$1.72M	$0.187	99.1

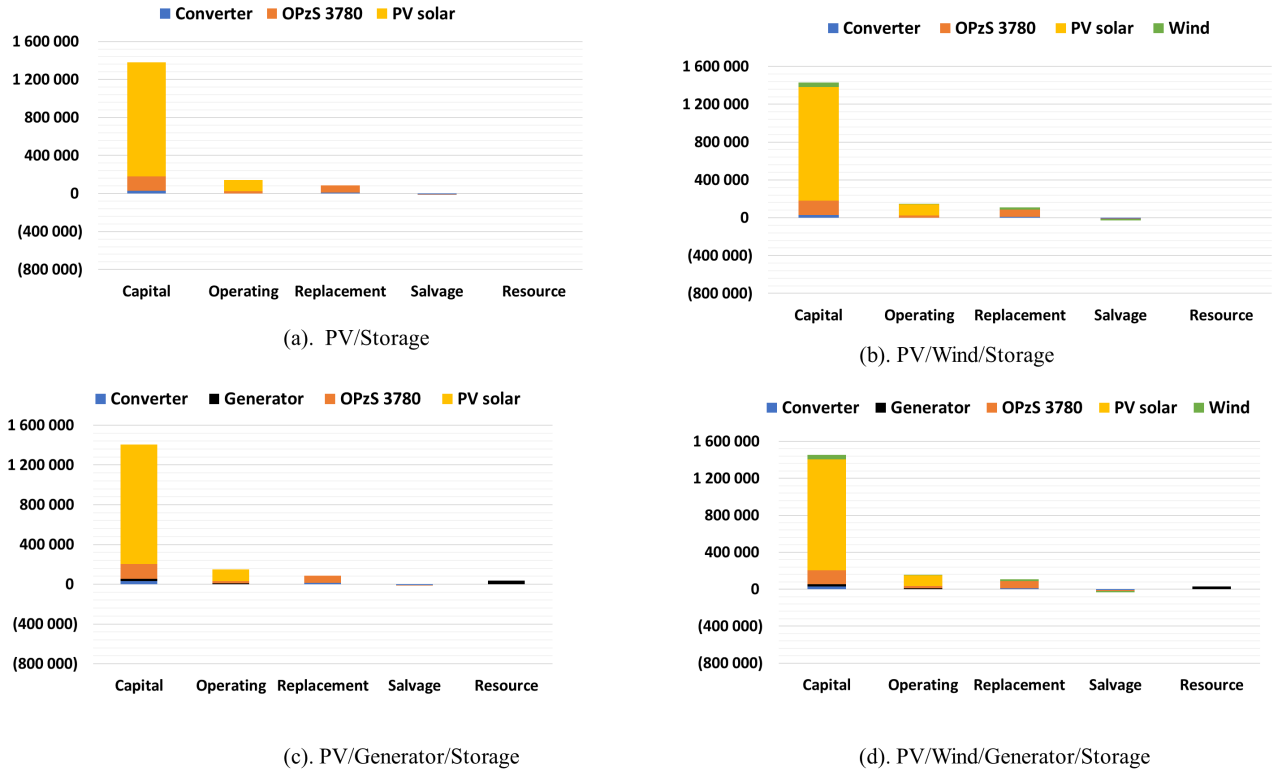

(a). PV/Storage

(b). PV/Wind/Storage

(c). PV/Generator/Storage

(d). PV/Wind/Generator/Storage

Figure 11. Cost summary of the project components of the four architectures.

7.1.1. Results of the Economic Evaluation of the Different Architectures

Based on the analyses, it has been determined that the cost of energy (COE) across all architectures is relatively similar, with only a 1% difference in the fraction of renewable energies used. To mitigate issues of power outages or lack of coverage during periods of low renewable energy availability, it is recommended to choose the reference architecture outlined in **Figure 11(d)**, which combines PV, wind, generator, and storage systems for optimal performance, self-consumption, and cost savings for the village.

7.1.2. Reference Architecture Result

As depicted in **Figure 11(a)**, the optimization results presented were obtained using HOMER Energy Pro software, indicating that the electricity demand of the village can be fulfilled by utilizing 1500 kW of PV and 2808 kWh of battery, with total annual operating costs of $13,903. To further reduce these costs, it is rec-

ommended to implement the reference architecture illustrated in Figure 11(d), which involves incorporating an extra 50 kW of diesel generator capacity and 10 kW of wind generation capacity. This modification would result in a decrease of the annual operating costs to $16,583, as demonstrated in Figure 12. The proposed investment is expected to yield a return on investment of 12.9 years.

Figure 13 presents the cash flow by component and the economic and chronological cash flow of the components over the 25-year lifespan of the project. The data reveals that many expenses were for diesel generator fuel, totaling $31958.21. For renewable energy, most of the spending was for operation and maintenance of photovoltaic solar panel components, followed by storage batteries and system maintenance costs.

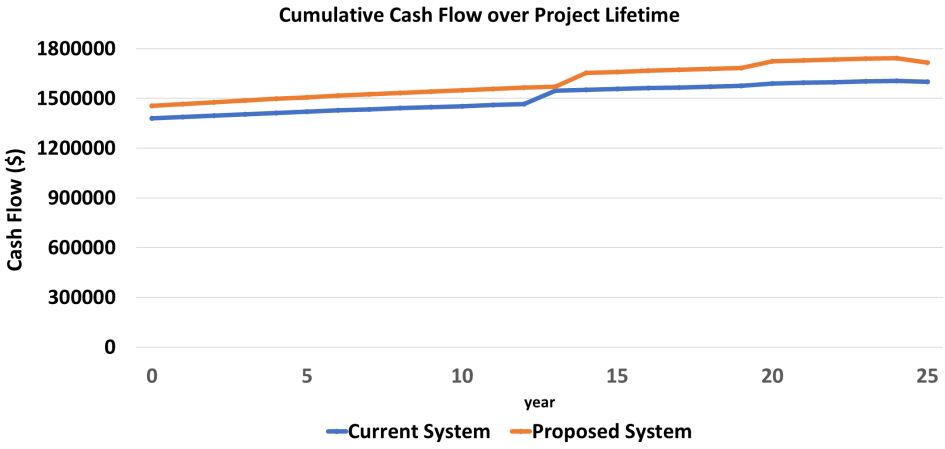

Figure 12. Cumulative cash flow over project lifetime.

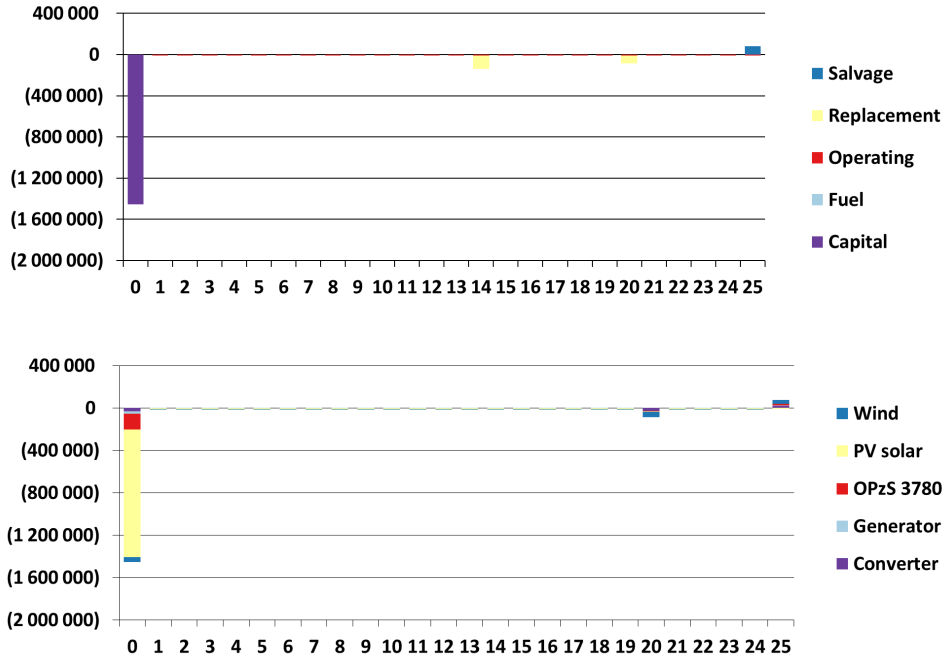

Figure 13. The economic and chronological cash flow of the components.

7.1.3. Electricity Generation

The proposed system for this microgrid, which requires an average daily consumption of 1603.60 kWh and peaks at 143.16 kW, utilizes various generation sources to meet the electrical load.

As depicted in Figure 14, the lion's share of electricity generation, amounting to 2,762,338 kWh annually or 99.2% of the total, originates from photovoltaic solar panels. In contrast, the wind turbine's contribution is relatively minor, delivering 16,841 kWh per year, equivalent to 0.6%. The diesel generator, reserved exclusively for backup during renewable energy downtimes, adds a mere 5183 kWh annually, representing a slender fraction of between 0.186% to 0.2% of the overall electricity output. This hybrid system's efficacy is underscored by the predominance of renewable sources in its energy mix, with 99.2% of its output being green. Remarkably, this configuration yields an energy surplus estimated at 2,125,344 kWh annually, translating to 76.3% of the total generation.

This system not only exemplifies the potential for sustainable energy solutions but also demonstrates the diminishing role of fossil fuels in modern energy strategies. By leveraging the inherent strengths of both solar and wind power, it achieves a remarkable balance between reliability and environmental stewardship. Moreover, the substantial energy surplus underscores the feasibility of transitioning to renewable sources without compromising on energy security or availability. This model serves as a beacon for future energy systems aiming for sustainability and resilience against the backdrop of global energy challenges.

As seen in Figure 15, a typical sunny day in the village of May 5th was chosen to demonstrate the performance of the chosen system. The results show a clear dominance of the solar photovoltaic system, with a peak power output of 1200 kW at noon when the sun is at its highest point. Additionally, the state of charge of the storage batteries is observed to vary between 50% - 100% throughout the day, further highlighting the effectiveness of the system.

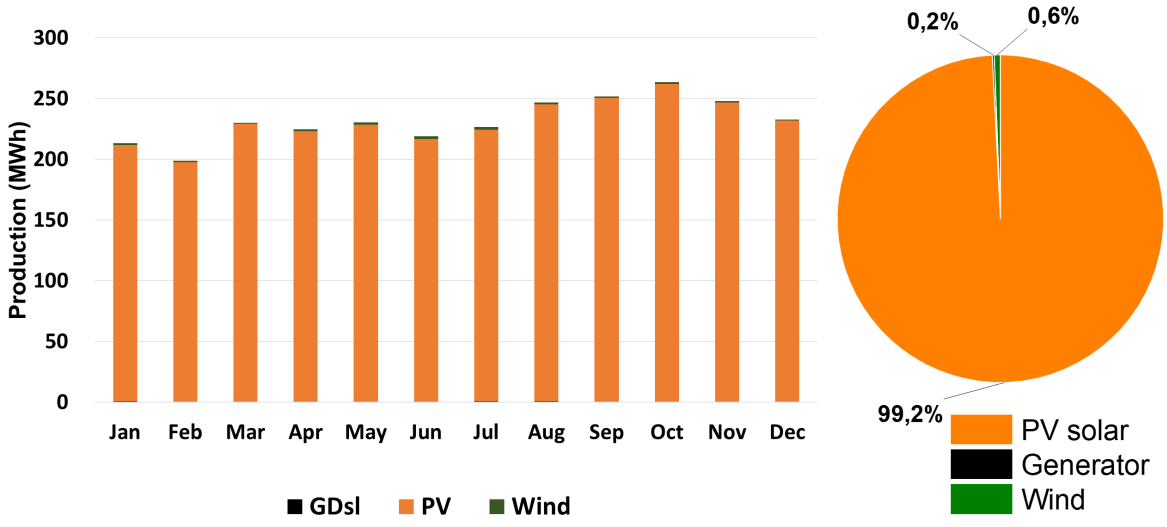

Figure 14. Electrical production of the hybrid system.

In Figure 16(a), the diesel generator is mostly inactive, with a power output that ranges from 0 kW to 50 kW, operating only during the night when the wind turbine's production is insufficient, and the storage batteries are depleted. The production of the solar photovoltaic system, as shown in Figure 16(b), is constant throughout the day, from 6am to 6pm, supplying electricity to the village with a power output that varies from 0 kW to 1500 kW. The wind turbine, as shown in Figure 16(c), operates throughout the day, producing a power output that ranges from 0 kW to 10 kW. In Figure 16(d), the state of charge of the storage batteries is crucial, with a deep discharge rate of 40% and a deep charge rate of 100% during the day, around 10am to 5pm, throughout the year.

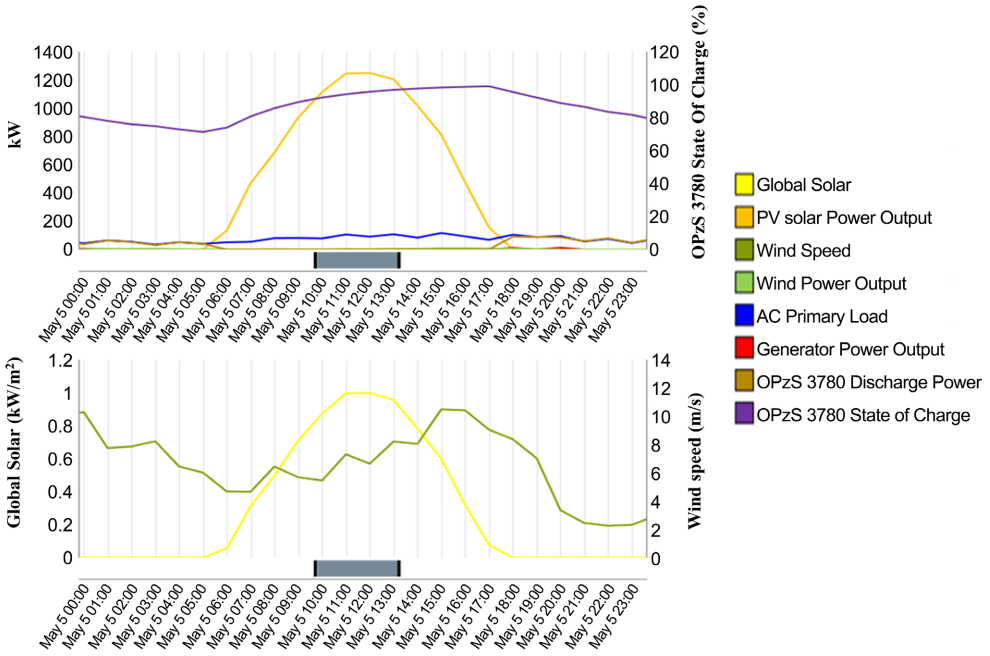

Figure 15. Production and weather situation for a typical day.

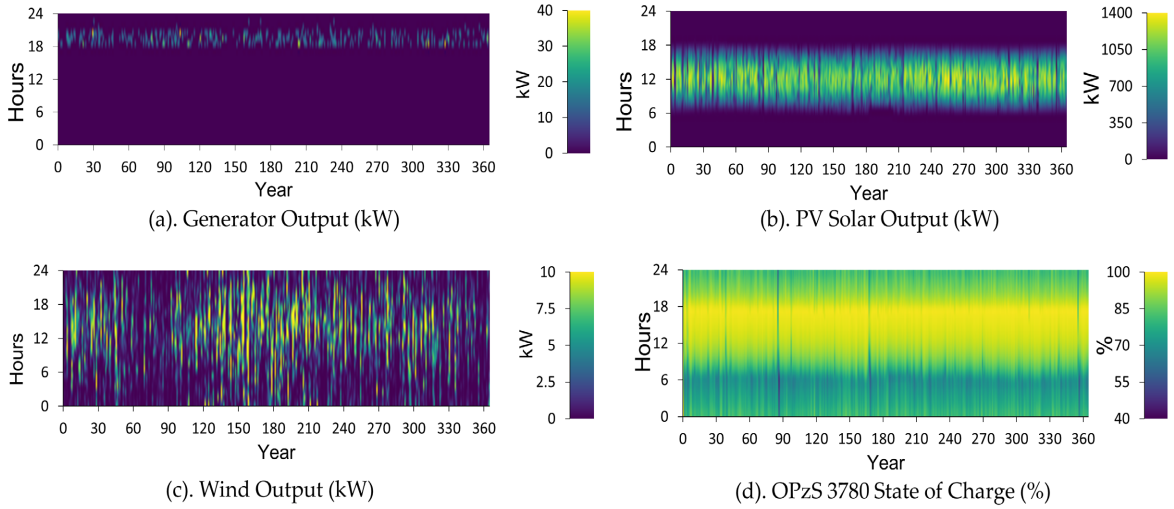

(a). Generator Output (kW)

(b). PV Solar Output (kW)

(c). Wind Output (kW)

(d). OPzS 3780 State of Charge (%)

Figure 16. Component production of hybrid system architecture.

7.2. Results by Sensitivity

Figure 17(a) and Figure 17(b), alongside Figure 18(a) and Figure 18(b), present a comprehensive analysis of the optimal system configuration, taking into account fuel costs and wind speed variables. Specifically, Figure 17(a) and Figure 17(b) detail the system's total net cost at varying diesel prices, \$0.5/L and \$1/L respectively, highlighting the financial dynamics under different fuel price scenarios. The analysis reveals that the PV/Battery system, a solution relying entirely on renewable energy, emerges as the preeminent option in terms of cost-effectiveness. Trailing this leader, the hybrid PV/Wind/GDsl/Battery system secures the second position, demonstrating a balanced integration of multiple energy sources. The GDsl/PV/Battery system occupies the third place, followed by the PV/Wind/Battery configuration, which, despite its renewable composition, ranks last in cost efficiency.

The span of the total net cost (NPC) for these systems, ranging from \$1,599,004 to \$2,281,352, underscores the influence of external factors such as global solar radiation and average wind speed on system economics.

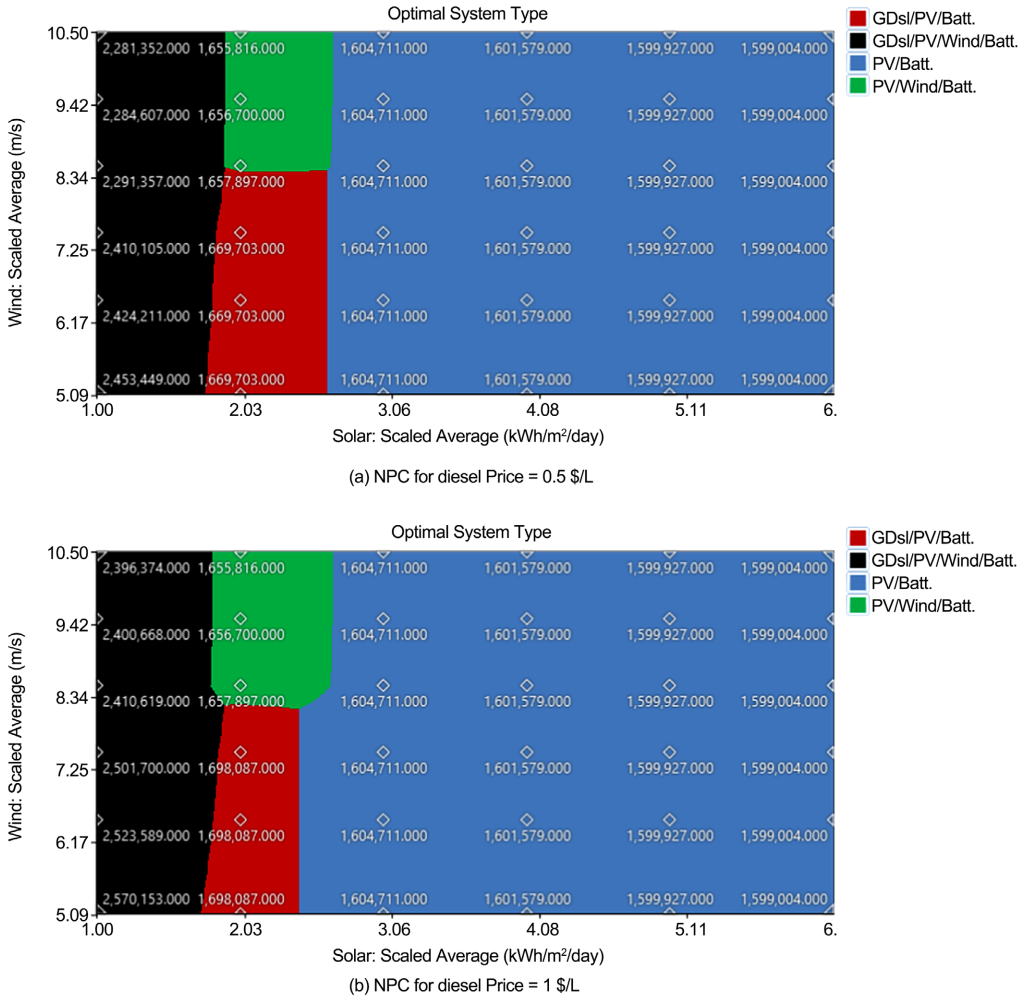

Figure 17. NPC with variation in diesel price.

This variability accentuates the critical role of environmental conditions in determining the optimal energy mix and system design. Additionally, this analysis serves as a testament to the evolving landscape of energy systems, where the integration of renewable resources is increasingly becoming a viable and cost-effective alternative to traditional fossil fuel-based setups.

By incorporating renewable energy sources, such systems not only offer a hedge against fluctuating fuel prices but also contribute to a reduction in carbon footprint, aligning with global sustainability goals. This insight into cost dynamics and system performance underlines the importance of strategic planning and investment in renewable energy technologies, setting a path for a more sustainable and economically feasible energy future.

The sensitivity analysis examined the impact of changes in fuel prices, wind speed and solar irradiation, allowing for an assessment of the robustness of system configurations to fluctuations in key parameters.

Figure 18(a) depicts the levelized cost of energy at a constant wind speed of 5.09 m/s, where the Photovoltaic/Battery (PV/Battery) system emerges as the most cost-effective option. It is closely followed by the integrated Photovoltaic/Wind/Generator Diesel/Battery (PV/Wind/GDsl/Battery) system, with the Generator Diesel/Photovoltaic/Battery (GDsl/PV/Battery) configuration ranking third in terms of cost efficiency. In contrast, Figure 18(b) examines the scenario when the wind speed is elevated to 8.5 m/s. Here, the PV/Battery system maintains its prominence as a cost-effective energy solution. Meanwhile, the GDsl/PV/Battery system becomes obsolete, and the Photovoltaic/Wind/Battery (PV/Wind/Battery) system emerges as a feasible alternative. This shift highlights the dynamic nature of renewable energy systems' economic viability, which significantly depends on environmental conditions. Notably, the increase in wind speed not only alters the competitive landscape among these systems but also underscores the importance of adaptability in optimizing the integration of renewable energy sources. As the reliance on renewable energy grows, understanding these dynamics becomes crucial for developing efficient, sustainable energy solutions tailored to specific environmental conditions.

On the other hand, the PV/Battery system is economically favorable, as it has a levelized cost of energy that ranges between $0.198/kWh. As seen in Figure 18(b), at a fixed wind speed of 8.5 m/s, the hybrid PV/Battery energy system is no longer present, and the Wind/PV/Battery combination becomes the most advantageous with a range of $0.175 to $0.267/kWh. This configuration shows that increasing the wind speed leads to a reduction in energy costs for the consumers and a reduction in diesel fuel consumption. The village inhabitants can potentially rely on 100% renewable energy when the wind speed reaches 8.5 m/s. As the wind speed increases, the contribution of renewable energy becomes more favorable, and the hybrid system works well with energy storage in batteries for later use. The PV/Battery system is considered to be the most suitable for this scenario.

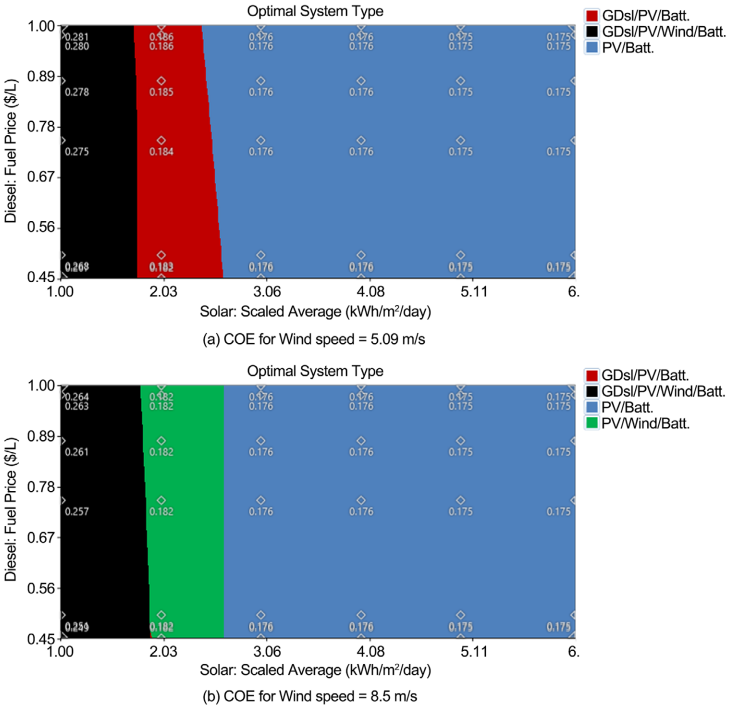

Figure 18. COE with variation in wind speed.

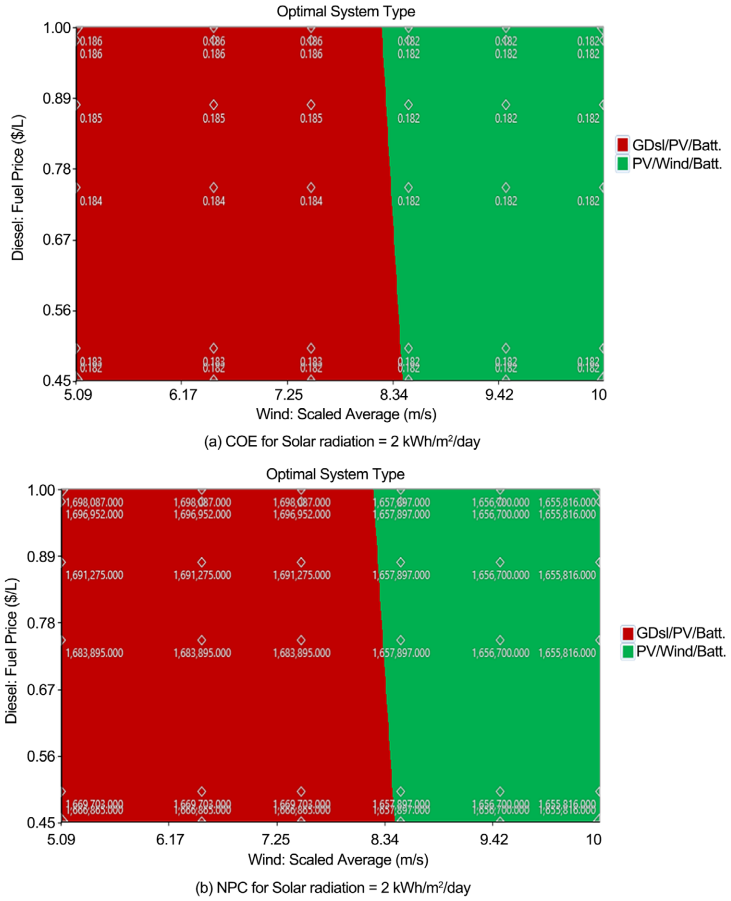

Figure 19. NPC and COE with fixed solar irradiance value.

The study was conducted with a fixed solar radiation of 2 kWh/m²/day (Figure 19), a fuel price of $1/L and a wind speed of 5.09 m/s. The results showed that the most dominant architecture of the system is the GDsl/PV/Battery configuration, with the potential for a 100% renewable architecture composed of PV/Wind/Battery. The cost of energy (COE) varies between $0.182/kWh and $0.186/kWh and the net present cost (NPC) varies between $1,555,816 and $1,698,087.

8. Gas Emission

Table 8 shows an estimated gas emission production of 5390,059 kg/year. In Figure 20, we see a maximum production of CO_2 at around 98.5%, an estimated value of 5311 kg/year and which is really negligible in terms of emissions. In second place we find carbon monoxide with a percentage of 0.6% or the value of 33.2 kg/year and in third place Nitrogen Oxides which also occupies 0.6% or 31.2 kg/year. The other gases are almost at 0%. Following this cost at, we can say that our project is good in terms of respect and protection of the environment. This respect for the environment is due to the fact that 99.1% of the energy produced comes from so-called green or renewable energy.

Table 8. The distribution of gas emissions.

Quantity	Value	Units
Carbon Dioxide	5311	kg/yr
Carbon Monoxide	33.2	kg/yr
Unburned Hydrocarbons	1.46	kg/yr
Particulate Matter	0.199	kg/yr
Sulfur Dioxide	13.0	kg/yr
Nitrogen Oxides	31.2	kg/yr
Total	5390.059	Kg/yr

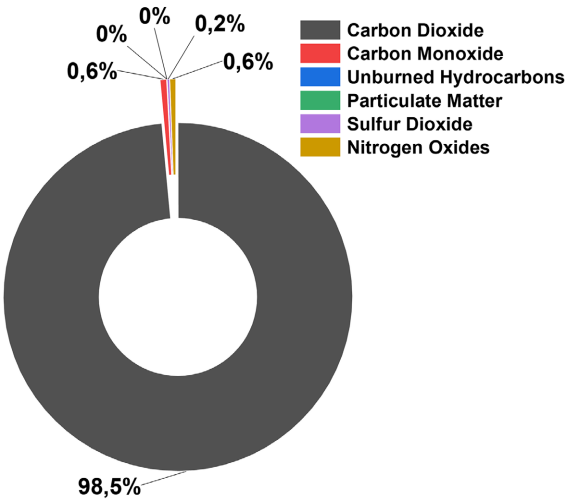

Figure 20. Share of gas emissions.

9. Conclusions and Prospects

In this research, an approach to providing power to a rural village in the Comoros was developed using the simulation tool HOMER Energy Pro. The proposed system includes a combination of a photovoltaic system, a wind turbine, a generator, and a storage battery. The study was carried out using meteorological data from the Comoros, including wind speed and solar irradiation, to optimize the design. The findings indicate that the optimal configuration of the system is a 100 kW converter, a 10 kW wind turbine, a PV field with a nominal capacity of 1500 kW and a 500-chain storage unit of OPzS 3780, resulting in a net total cost of $1,716,229, an operating cost of $16,583.43/year and a cost of energy sales of $0.1871/kWh. Additionally, the majority of electricity production is expected to come from the solar PV system at 2,762,338 kWh/year or 99.2%, followed by wind at 16,841 kWh/year or 0.6% and the diesel generator with a value of 5183 kWh/year or 0.186% - 0.2% of electricity production. This proposed system is expected to effectively meet the needs of the village as it relies heavily on renewable energy sources, with an estimated surplus of 2,125,344 kWh/year or 76.3%. This surplus energy can be sold to the national electricity production company in the Comoros, SONELEC, and be reinjected into the electricity network, creating savings for the community. This surplus can also be used to fund other community projects that have been hindered due to energy shortages. Additionally, this excess energy can be used to provide electricity to other villages in the commune of Sada Djoulamlima, or even the entire northern region of Grande Comore. The results of this study indicate that solar resources in the village of Koua have a strong potential compared to wind power, making it the primary energy source for the community. This work will not only contribute to the protection of the environment and the fight against climate change but also allow this remote village to be self-sufficient and autonomous in terms of electrical energy, which will contribute to its socio-economic development.

Given the limited budget and lack of government funding for the project, we propose to the Comorian government to conduct feasibility and techno-economic studies for residential self-consumption in this area using hybrid photovoltaic thermal (PV/T) systems to meet the needs of households for both water and electricity. This alternative is more cost-effective and can address the urgent need for electricity in the country while larger community projects are being developed.

Acknowledgements

This work has been supported by the University of Lorraine's "DreAM" excellence grant program, project LUE GRADUATE - DREAM 8. The authors thank the leaders of this project.

Conflicts of Interest

The authors declare no conflicts of interest regarding the publication of this paper.

References

[1] Ma, W.W., Rasul, M.G., Liu, G., Li, M. and Tan, X.H. (2016) Climate Change Impacts on Techno-Economic Performance of Roof PV Solar System in Australia. *Renewable Energy*, **88**, 430-438. https://doi.org/10.1016/j.renene.2015.11.048

[2] Vidal, Y., Acho, L., Luo, N., Zapateiro De La Hoz, M.F. and Pozo, F. (2010) Power Control Design for Variable-Speed Wind Turbines.

[3] Touili, S., Alami Merrouni, A., El Hassouani, Y., Amrani, A. and Rachidi, S. (2020) Analysis of the Yield and Production Cost of Large-Scale Electrolytic Hydrogen from Different Solar Technologies and under Several Moroccan Climate Zones. *International Journal of Hydrogen Energy*, **45**, 26785-26799. https://doi.org/10.1016/j.ijhydene.2020.07.118

[4] IEA (n.d.) Perspectives Énergétiques Mondiales 2019, World Energy Outlook—Topics. https://iea.blob.core.windows.net/assets/98909c1b-aabc-4797-9926-35307b418cdb/WEO2019-free.pdf

[5] IEA (n.d.) Perspectives Énergétiques Mondiales 2020, World Energy Outlook—Topics. https://iea.blob.core.windows.net/assets/a72d8abf-de08-4385-8711-b8a062d6124a/WEO2020.pdf

[6] Norouzi, N., Bozorgian, A. and Dehghani, M.A. (2020) Best Option of Investment in Renewable Energy: A Multicriteria Decision-Making Analysis for Iranian Energy Industry. *Journal of Environmental Assessment Policy and Management*, **22**, Article ID: 2250001. https://doi.org/10.1142/S1464333222500016

[7] Norouzi, N. (2021) The Pahlev Reliability Index: A Measurement for the Resilience of Power Generation Technologies versus Climate Change. *Nuclear Engineering and Technology*, **53**, 1658-1663. https://doi.org/10.1016/j.net.2020.10.013

[8] Krohn, S., Morthorst, P.-E. and Awerbuch, S. (N.D.) The Economics of Wind Energy.

[9] Johnson, L. (2014) Geographies of Securitized Catastrophe Risk and the Implications of Climate Change. *Economic Geography*, **90**, 155-185. https://doi.org/10.1111/ecge.12048

[10] Aguilar, M.M. (N.D.) Production de Biobutanol A Partir de Lignocellulose: Un Nouveau Procede Thermochimique.

[11] Aguilar-Jimenez, J.A., Hernandez-Callejo, L., Alonso-Gomez, V., Velazquez, N., Lopez-Zavala, R., Acuña, A. and Mariano-Hernandez, D. (2020) Techno-Economic Analysis of Hybrid PV/T Systems under Different Climate Scenarios and Energy Tariffs. *Solar Energy*, **212**, 191-202. https://doi.org/10.1016/j.solener.2020.10.079

[12] Mohd Noor, M.S., Adzis, Z., Arief, Y.Z. and Muhamad, N.A. (2016) Feasibility Analysis of Stand-Alone Renewable Energy Supply for Telecommunication Tower Using Homer. *Applied Mechanics and Materials*, **818**, 223-227. https://doi.org/10.4028/www.scientific.net/AMM.818.223

[13] Gonzalez-Salazar, M. and Poganietz, W.R. (2021) Evaluating the Complementarity of Solar, Wind and Hydropower to Mitigate the Impact of El Niño Southern Oscillation in Latin America. *Renewable Energy*, **174**, 453-467. https://doi.org/10.1016/j.renene.2021.04.048

[14] Graabak, I. and Korpås, M. (2016) Balancing of Variable Wind and Solar Production in Continental Europe with Nordic Hydropower—A Review of Simulation Studies. *Energy Procedia*, **87**, 91-99.

https://doi.org/10.1016/j.egypro.2015.12.362

[15] Yao, Y., Xu, J.-H. and Sun, D.-Q. (2021) Untangling Global Levelised Cost of Electricity Based on Multi-Factor Learning Curve for Renewable Energy: Wind, Solar, Geothermal, Hydropower and Bioenergy. *Journal of Cleaner Production*, **285**, Article ID: 124827. https://doi.org/10.1016/j.jclepro.2020.124827

[16] Thirunavukkarasu, M. and Sawle, Y. (2021) A Comparative Study of the Optimal Sizing and Management of Off-Grid Solar/Wind/Diesel and Battery Energy Systems for Remote Areas. *Frontiers in Energy Research*, **9**, Article ID: 752043. https://www.frontiersin.org/articles/10.3389/fenrg.2021.752043 https://doi.org/10.3389/fenrg.2021.752043

[17] Maoulida, F., Rabah, D., Ganaoui, M.E. and Aboudou, K.M. (2021) PV-Wind-Diesel System for Energy Supply on Remote Area Applied for Telecommunication Towers in Comoros. *Open Journal of Energy Efficiency*, **10**, 50-72. https://doi.org/10.4236/ojee.2021.102004

[18] Maoulida, F., Aboudou, K.M., Djedjig, R. and El Ganaoui, M. (n.d.) Feasibility Study for a Hybrid Power Plant (PV-Wind-Diesel-Storage) Connected to the Electricity Grid. *Fluid Dynamics & Materials Processing*, **18**, 1607-1617.

[19] Garg, V.K. and Sharma, S. (N.D.) Techno-Economic Analysis of a Microgrid for a Small Community. In: Marriwala, N., *et al*., Eds., *Soft Computing for Intelligent Systems*, Springer, Berlin, 505-517. https://link.springer.com/chapter/10.1007/978-981-16-1048-6_40

[20] Olatomiwa, L., Mekhilef, S., Ismail, M.S. and Moghavvemi, M. (2016) Energy Management Strategies in Hybrid Renewable Energy Systems: A Review. *Renewable and Sustainable Energy Reviews*, **62**, 821-835. https://doi.org/10.1016/j.rser.2016.05.040

[21] Kassim, M., Fahad, M. and El Ganaoui, M. (2020) Pv-Wind Hybrid Energy System for Application of Building in Rural Areas in Comoros.

[22] Fahad, M., Kassim, M., Rakoto, J. and El Ganaoui, M. (2020) Dimensionnement d'un systeme hybride pv/generateur diesel pour l'alimentation electrique d'un pylone de telecommunication aux comores.

[23] Aboudou, K.M. and Ganaoui, M.E. (2019) Design of a Hybrid System for Rural Area Electricity Supply in Comoros. *Journal of Power and Energy Engineering*, **7**, 59-78. https://doi.org/10.4236/jpee.2019.72005

[24] Kassim, M. and El Ganaoui, M. (2018) Design of Hybrid Power System for a Power Supply in Rural Areas in Comoros.

[25] IRENA (2021) World Energy Transitions Outlook: 1.5 ˚C Pathway. International Renewable Energy Agency, Abu Dhabi. https://www.irena.org/publications

[26] Agence Internationale des Energies Renouvelables (n.d.) Renewable Capacity Statistics 2019.

[27] (2018) Irena afrique, l'afrique et les energies renouvelables: La voie vers la croissance durable. https://publications/2013/feb/lafrique-et-les-nergies-renouvelables--la-voie-vers-la-croissance-durable

[28] Burke, P.J. and Kurniawati, S. (2018) Electricity Subsidy Reform in Indonesia: Demand-Side Effects on Electricity Use. *Energy Policy*, **116**, 410-421. https://doi.org/10.1016/j.enpol.2018.02.018

[29] Gouvernement de L'Union des Comores (2020) Rapport national volontaire de l'union des comores au forum politique de haut niveau sur le developpement durable.

[30] Fahad, M., Kassim, M., Djedjig, R. and Ganaoui, M. (2022) Feasibility Study for a Hybrid Power Plant (PV-Wind-Diesel-Storage) Connected to the Electricity Grid. *Fluid Dynamics and Materials Processing*, **18**, 1607-1617. https://doi.org/10.32604/fdmp.2022.023199

[31] Maoulida, F. (2020) Developpement d'un systeme hybride de generation d'energie en site isole pour la telecommunication et realisation d'un regulateur de charge solaire, memoire de master 2, d'ingenierie en énergies renouvelables, universite d'antananarivo.

[32] Alturki, F.A. and Dayil, A.B. (2020) Techno-Economic Evaluation and Optimization of Grid Connected PV and Wind Generating System for Riyadh City. *Journal of Power and Energy Engineering*, **8**, 46-63. https://doi.org/10.4236/jpee.2020.812004

[33] Mandal, S., Das, B.K. and Hoque, N. (2018) Optimum Sizing of a Stand-Alone Hybrid Energy System for Rural Electrification in Bangladesh. *Journal of Cleaner Production*, **200**, 12-27. https://doi.org/10.1016/j.jclepro.2018.07.257

[34] Alsamamra, H.R. and Shoqeir, J.A.H. (2020) Assessment of Wind Power Potential at Eastern-Jerusalem, Palestine. *Open Journal of Energy Efficiency*, **9**, 131-149. https://doi.org/10.4236/ojee.2020.94009

[35] Weinand, J.M., Scheller, F. and McKenna, R. (2020) Reviewing Energy System Modelling of Decentralized Energy Autonomy. *Energy*, **203**, Article ID: 117817. https://doi.org/10.1016/j.energy.2020.117817

[36] Yang, Y., Javanroodi, K. and Nik, V.M. (2022) Climate Change and Renewable Energy Generation in Europe—Long-Term Impact Assessment on Solar and Wind Energy Using High-Resolution Future Climate Data and Considering Climate Uncertainties. *Energies*, **15**, Article No. 302. https://doi.org/10.3390/en15010302

[37] Kassim, M. and El Ganaoui, M. (2019) Design of a Hybrid System for Rural Area Electricity Supply in Comoros. *Journal of Power, and Energy Engineering*, **7**, 59-78. https://doi.org/10.4236/jpee.2019.72005

[38] Halabi, L.M., Mekhilef, S., Olatomiwa, L. and Hazelton, J. (2017) Performance Analysis of Hybrid PV/Diesel/Battery System Using HOMER: A Case Study Sabah, Malaysia. *Energy Conversion and Management*, **144**, 322-339. https://doi.org/10.1016/j.enconman.2017.04.070

[39] Riayatsyah, T.M.I., Geumpana, T.A., Fattah, I.M.R. and Mahlia, T.M.I. (2022) Techno-Economic Analysis of Hybrid Diesel Generators and Renewable Energy for a Remote Island in the Indian Ocean Using HOMER Pro. *Sustainability*, **14**, Article No. 9846. https://doi.org/10.3390/su14169846

[40] Geyken, C. (N.D.) Analysis to Achieve a High Penetration of Renewable Energies in MW-Scale Electricity Microgrids with the Case Study of an Island in the Pacific.

[41] Dufo-LÓPez, R. and Bernal-AgustÍN, J.L. (2005) Design and Control Strategies of PV-Diesel Systems Using Genetic Algorithms. *Solar Energy*, **79**, 33-46. https://doi.org/10.1016/j.solener.2004.10.004

[42] Chao, J.L. (2021) Experts' Predictions for Future Wind Energy Costs Drop Significantly. News Center. https://newscenter.lbl.gov/2021/04/15/experts-predictions-for-future-wind-energy-costs-drop-significantly/

[43] Homer Energy (n.d.) HOMER—Logiciel de conception de systemes de generation hybrides renouvelables et distribues. https://www.homerenergy.com/

[44] Manmadharao, S., Chaitanya, S.N.V.S.K., Venkateswara Rao, B. and Srinivasarao, G. (2019) Design and Optimization of Grid Integrated Solar Energy System Using

HOMER GRID Software. 2019 *Innovations in Power and Advanced Computing Technologies* (*I-PACT*), Vellore, 22-23 March 2019, 1-5. https://doi.org/10.1109/i-PACT44901.2019.8960118

[45] Ghatak, A., Alfred, R.B. and Singh, R.R. (2021) Optimization for Electric Vehicle Charging Station Using Homer Grid. 2021 *Innovations in Power and Advanced Computing Technologies* (*I-PACT*), Kuala Lumpur, 27-29 November 2021, 1-7. https://doi.org/10.1109/i-PACT52855.2021.9696626

[46] Sen, R. and Bhattacharyya, S.C. (2014) Off-Grid Electricity Generation with Renewable Energy Technologies in India: An Application of HOMER. *Renewable Energy*, **62**, 388-398. https://doi.org/10.1016/j.renene.2013.07.028

[47] Shahzad, M.K., Zahid, A., Ur Rashid, T., Rehan, M.A., Ali, M. and Ahmad, M. (2017) Techno-Economic Feasibility Analysis of a Solar-Biomass Off Grid System for the Electrification of Remote Rural Areas in Pakistan Using HOMER Software. *Renewable Energy*, **106**, 264-273. https://doi.org/10.1016/j.renene.2017.01.033

[48] Bahramara, S., Moghaddam, M.P. and Haghifam, M.R. (2016) Optimal Planning of Hybrid Renewable Energy Systems Using HOMER: A Review. *Renewable and Sustainable Energy Reviews*, **62**, 609-620. https://doi.org/10.1016/j.rser.2016.05.039

[49] Ahmad, J., Imran, M., Khalid, A., Iqbal, W., Ashraf, S.R., Adnan, M., Ali, S.F. and Khokhar, K.S. (2018) Techno Economic Analysis of a Wind-Photovoltaic-Biomass Hybrid Renewable Energy System for Rural Electrification: A Case Study of Kallar Kahar. *Energy*, **148**, 208-234. https://doi.org/10.1016/j.energy.2018.01.133

[50] Wikipedia (2020) Position geographique des comores. https://fr.wikipedia.org

[51] Wikipedia (2020) Demographie des comores (Pays). https://fr.wikipedia.org

[52] UNECA BSR-EA (2018) Gouvernement de l'union des comores, developpement des statistiques du bilan energetique et d'un modele de systeme energetique pour l'union des comores. https://archive.uneca.org

[53] Boukhchana, Y., Fellah, A. and Ben Brahim, A. (2011) Modelisation de la phase generation d'un cycle de refrigeration par absorption solaire a fonctionnement intermittent. *International Journal of Refrigeration*, **34**, 159-167. https://doi.org/10.1016/j.ijrefrig.2010.08.002

[54] (2020) Solargis des Comores, Solar Resource Maps of Comoros. https://solargis.com/maps-and-gis-data/download/comoros

[55] Benalcazar, P., Suski, A. and Kamiński, J. (2020) Optimal Sizing and Scheduling of Hybrid Energy Systems: The Cases of Morona Santiago and the Galapagos Islands. *Energies*, **13**, Article No. 3933. https://doi.org/10.3390/en13153933

[56] El-Houari, H., Allouhi, A., Rehman, S., Buker, M.S., Kousksou, T., Jamil, A. and El Amrani, B. (2019) Design, Simulation, and Economic Optimization of an Off-Grid Photovoltaic System for Rural Electrification. *Energies*, **12**, Article No. 4735. https://doi.org/10.3390/en12244735

[57] Said, Z., Arora, S. and Bellos, E. (2018) A Review on Performance and Environmental Effects of Conventional and Nanofluid-Based Thermal Photovoltaics. *Renewable and Sustainable Energy Reviews*, **94**, 302-316. https://doi.org/10.1016/j.rser.2018.06.010

[58] Mehta, S. and Basak, P. (2022) A Novel Design Economic Assessment and Fuzzy-Based Technical Validation of an Islanded Microgrid: A Case Study on Load Model of Kibber Village in Himachal Pradesh. *International Transactions on Electrical Energy Systems*, **2022**, e9639253. https://doi.org/10.1155/2022/9639253

[59] Homer Energy Pro (n.d.) How HOMER Creates the Generator Efficiency Curve.

https://support.ul-renewables.com/homer-manuals-pro/generator_fuel_curve_slope.html

[60] Kassim, M., Fahad, M. and El Ganaoui, M. (2020) Pv-Wind Hybrid Energy System for Application of Building in Rural Areas in Comoros.

[61] Homer Energy Pro (n.d.) How HOMER Calculates the PV Array Power Output. https://support.ul-renewables.com/homer-manuals-pro/how_homer_calculates_the_pv_array_power_output.html

[62] Brihmat, F. and Mekhtoub, S. (N.D.) PV Cell Temperature/PV Power Output Relationships Homer Methodology Calculation.

[63] Haffaf, A., Lakdja, F., Meziane, R. and Abdeslam, D.O. (2021) Study of Economic and Sustainable Energy Supply for Water Irrigation System (WIS). *Sustainable Energy, Grids and Networks*, **25**, Article ID: 100412. https://doi.org/10.1016/j.segan.2020.100412

[64] Lare, Y., Sagna, K. and Razak Ali-Tagba, A. (2021) Optimal Design and Performance Analysis of a Grid Connected Photovoltaic System in Togo. *AJER*, **9**, 56-74. https://doi.org/10.12691/ajer-9-1-6

[65] Homer Energy Pro (n.d.) How HOMER Calculates Wind Turbine Power Output. https://support.ul-renewables.com/homer-manuals-pro/wind_resource_variation_with_height.html

[66] Delannoy, L., Puri, S., Perera, A.T.D., Coccolo, S., Mauree, D. and Scartezzini, J.-L. (2018) Climate Impact and Energy Sustainability of Future European Neighborhoods. 2018 5*th International Symposium on Environment-Friendly Energies and Applications* (*EFEA*), Rome, 24-26 September 2018, 1-6. https://doi.org/10.1109/EFEA.2018.8617066

[67] Homer Energy Pro (n.d.) Battery Bank Life. https://support.ul-renewables.com/homer-manuals-pro/how_homer_calculates_the_maximum_battery_charge_power.html

[68] Homer Energy Pro (n.d.) Levelized Cost of Energy. https://support.ul-renewables.com/homer-manuals-pro/levelized_cost_of_energy.html

[69] El-Houari, H., Allouhi, A., Rehman, S., Buker, M.S., Kousksou, T., Jamil, A. and El Amrani, B. (2020) Feasibility Evaluation of a Hybrid Renewable Power Generation System for Sustainable Electricity Supply in a Moroccan Remote Site. *Journal of Cleaner Production*, **277**, Article ID: 123534. https://doi.org/10.1016/j.jclepro.2020.123534

[70] Homer Energy Pro (n.d.) Annualized Cost. https://support.ul-renewables.com/homer-manuals-pro/annualized_cost.html

Abbreviations

HOMER	Hybrid Optimization Model for Electric Renewable
HPS	Hybrid Power System
IEA	International Energy Agency
PV	Photovoltaic
SONELEC	National electricity production company in the Comoros
ANACEM	National Agency of Civil Aviation and Meteorology
PV/T	Photovoltaic Thermal